Multiple-Pion Production by 2-BeV π^-*

P. H. SATTERBLOM,† W. D. WALKER, AND A. R. ERWIN
Physics Department, University of Wisconsin, Madison, Wisconsin
(Received 25 September 1963; revised manuscript received 2 December 1963)

A report is given of a study of pion-proton interactions in a liquid-hydrogen bubble chamber. A 2.1-BeV/c negative pion beam incident upon a 14-in.-diam chamber caused interactions from which those with four charged secondaries were selected and measured. Fits were attempted to the following final states: $3\pi+p$, $3\pi+p+\pi^0$, and $4\pi+n$. By normalizing to a total cross section of 35.7 mb, the partial cross sections for the above-listed final states are found to be 1.67 ± 0.08, 1.17 ± 0.06, and 0.37 ± 0.02 mb. The $3\pi+p$ reaction was found to be dominated by the production of the $\frac{3}{2}$–$\frac{3}{2}$ pion-nucleon isobar. The cross section for this process is 0.53 ± 0.05 mb. Evidence for the eta and omega mesons was found in the $3\pi+p+\pi^0$ final state. Their cross sections are 0.037 ± 0.015 and 0.26 ± 0.035 mb, respectively. A Dalitz plot for eta decays is presented. Evidence is given for a double peak in the neutral two-pion mass spectrum for $3\pi+p$ and $4\pi+n$ events. The peaks coincide with those attributed to the rho meson in other experiments. The second of the two peaks corresponds well with the mass of the ω^0. A branching ratio of $\omega^0\to 2\pi/\omega^0\to 3\pi$ is found to be >0.1. An attempt is made to calculate the pion-pion cross section by isolating events with low momentum transfer to the isobar. In the various processes, enhancement is found in the nucleon $+2\pi$ mass spectra corresponding to the $T=\frac{3}{2}$ state of mass 1920 MeV. It is proposed that the elementary crossed diagram can explain these effects.

I. INTRODUCTION

THE discovery of pion-nucleon isobars, multiple-pion resonances and the proposal of theories to account for meson production, have brought attention to the phenomena of multiple pion production. The advent of accelerators with the ability to produce high-energy pion beams has made it now possible to study interactions wherein multiple processes may dominate. Early experiments in the 1-BeV region on pion-nucleon interactions performed with cloud chambers and emulsions were primarily concerned with elastic and single-pion production events.[1,2] A model for pion production in pion-nucleon collisions has been formulated by Lindenbaum and Sternheimer which assumes that all reactions proceed through excitations of the $T=J=\frac{3}{2}$ isobar.

More recently, interest has shifted to events with higher multiplicity in order to study the effects of the newly discovered multiple-pion resonances. Experiments on single production have yielded information concerning a peak in the pion-pion cross section at a di-pion mass of 750 MeV, the so-named rho isovector meson, which has a full-width of about 150 MeV.[3] Reactions wherein at least three mesons are produced have established the two isoscalar omega[4] and eta[5] three pion resonances. As additional experiments are performed in this energy region on multiple-pion production, more candidates for the title of resonance are being reported.

Some of these resonances are needed in one or more of the theoretical models which have been proposed. Sakurai's vector theory of strong interactions[6] predicts an isovector meson of $J=1^{-+}$ and an isoscalar meson of $J=1^{--}$. The "8-fold way" theory of Gell-Mann[7] uses the two above-mentioned states of Sakurai along with an isoscalar meson, having $J=0^{-+}$. These three states fit the observed ρ, ω, and η mesons.

It is of interest, therefore, to attempt to experimentally relate the multiple-pion production mechanism at 2.0 BeV to one or more of these new quasiparticles. A report will be given here of an experiment in which this attempt was made.

Within a fiducial volume of a 14-in.-diam liquid-hydrogen bubble chamber having a 17.15-kilogauss magnetic field, 2500 negative pion-on-proton events with four charged secondaries were obtained. The pion beam had a momentum of 2.10 ± 0.04 BeV/c. These events were examined for examples of the following reactions.

1. $\pi^-+p\to\pi^-+p+\pi^-+\pi^+$.
2. $\pi^-+p\to\pi^-+p+\pi^-+\pi^+\pi^0$.
3. $\pi^-+p\to\pi^-+n+\pi^-+\pi^+\pi^+$.

Measurements were made of the events by means of digitized projection equipment and computations carried out on an IBM 704. A somewhat modified form of the "Guts"[8] kinematic fitting subroutine formed the basis of the analysis program which, along with range

* Supported in part by a contract with the U. S. Atomic Energy Commission and by grants from the Wisconsin Alumni Research Foundation.
† Part of a thesis submitted by P. H. Satterblom.
[1] L. M. Eisberg, W. B. Fowler, R. M. Lea, W. D. Shephard, R. P. Shutt, A. M. Thorndike, and W. L. Whittemore, Phys. Rev. **97**, 797 (1955).
[2] W. D. Walker and J. Crussard, Phys. Rev. **98**, 1416 (1955).
[3] A. R. Erwin, R. H. March, W. D. Walker, and E. West, Phys. Rev. Letters **6**, 628 (1961).
[4] B. C. Maglic, L. W. Alvarez, A. H. Rosenfeld, and M. L. Stevenson, Phys. Rev. Letters **7**, 178 (1961).
[5] A. Pevsner, R. Kraemer, M. Nussbaum, C. Richardson, P. Schlein, R. Strand, T. Toohig, M. Block, A. Engler, R. Cessaroli, and C. Meltzer, Phys. Rev. Letters **7**, 421 (1961).
[6] J. J. Sakurai, Ann. Phys. **11**, 1 (1960).
[7] M. Gell-Mann, Phys. Rev. **125**, 1067 (1962).
[8] J. P. Berge, F. T. Schmitz, and H. D. Taft, University of California, Lawrence Radiation Laboratory Report No. UCRL-9097, 1960 (unpublished).

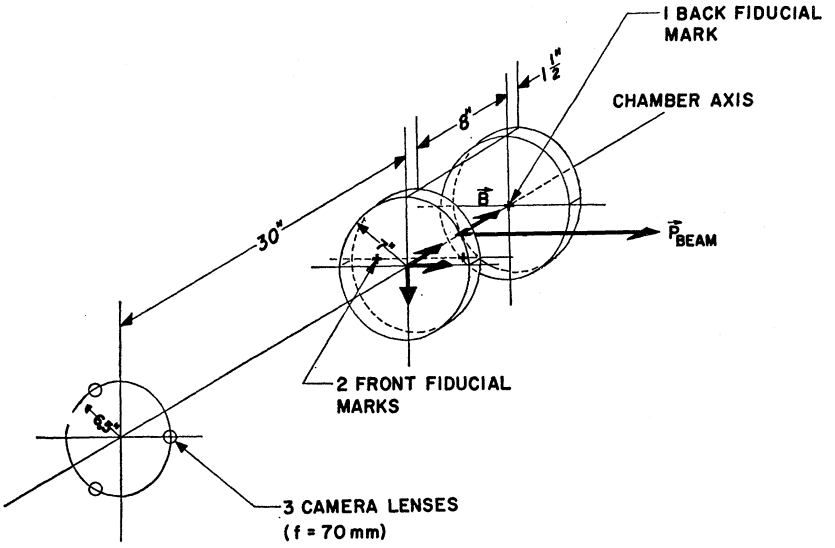

FIG. 1. Optical layout for chamber.

and ionization measurements, indicated fits to the following numbers of final states:

1116 cases of reaction 1,

571 cases of reaction 2,

246 cases of reaction 3.

The remaining nonanalyzable events can be taken to be examples of two prongs with Dalitz pairs, events with higher multiplicity, and events with poor measurements.

II. METHOD

A. Chamber

This experiment was performed at the Cosmotron using the 14-in. Adair liquid-hydrogen bubble chamber. The active volume of this chamber is cylindrical with a 14-in. inside diam and an 8-in. inside depth (see Fig. 1). The magnetic field is directed along the cylinder axis and has a value determined by previous calibration as well as by fitting the Q value of Λ^0 decays. The central field value was 17.15 kG. with a fluctuation of ± 86 G.

35-mm photographs were taken by three cameras located as indicated in Fig. 1.

B. Beam

The experimental arrangement of bending and focusing magnets designed by A. R. Erwin is given in Fig. 2 (shielding has been omitted). The Cosmotron external beam III was focused onto a lead target creating secondaries which were momentum analyzed by two bending magnets and a double collimation system. The magnet array was designed to give a momentum of 2.1 BeV/c. The distance along the beam path from the target to the chamber was 34.2 m.

The momentum and resolution of the beam were determined in two ways. First, momenta of tracks traversing the entire chamber, about 35 cm, were measured, and second, the beam momentum required to fit known cases of Λ^0, K^0 production was calculated. The first method gives an indication of the momentum and spread dependent upon errors inherent in the measuring process, whereas the second method is more exact, depending only on the ability to measure angles between tracks, the ability to identify Λ^0, K^0 events and errors in the Λ^0 and K^0 mass values. The momentum determined in this latter manner and used in this analysis was 2.10 ± 0.04 BeV/c. As a check on the validity of this beam-momentum assignment and as an indication of the beam spread a plot was made of the fitted beam momenta for four constraint fits to the $3\pi+p$ final state. This plot has its peak between 2.09 and 2.10 BeV/c with a full width at half-maximum of 40 MeV/c.

Muon and electron contamination in the beam has been estimated by scanning for and measuring the momentum of "knock-on" electrons from beam tracks.[9] The maximum contaminations are 6% for muons and $\frac{1}{2}$% for electrons.

C. Scanning

Area scanning was used to locate frames containing events with four charged secondaries.

The fiducial volume for usable events was defined by the following criteria:

1. The vertex of the event must be more than 5 cm from the front or back glass. This gives 10 cm of effective depth.

2. The beam track must be longer than 2 cm to accurately determine its direction cosines.

3. The vertex of the event must be at least 15 cm from the exit side of the chamber. Assuming that the maximum measuring-machine setting error is 50μ or $\frac{1}{2}$

[9] G. Hoyer, University of Wisconsin (private communication).

of the track width, the resulting momentum error in a 1.5-BeV/c track is 70 MeV/c.

4. No track that leaves the chamber through the front or back windows can have a projected range of less than 5 cm in two or more views.

By comparing the results of various personnel, the scanning efficiency was found to be nearly 100% for events within the fiducial volume.

D. Measuring

The measuring machines used were digitized projectors. Chamber photographs were projected onto a viewing screen moveable by digitized lead screws to which were attached mechanical encoders defining the rectangular coordinate array. The coordinates of at least five points along each track were punched onto IBM cards along with the necessary identifying information.

In the case that the track stopped in the liquid hydrogen, a special note was made and the last measured point was taken at the end of the track regardless of the sagitta length. In the subsequent analysis of the event, the momentum given by range-momentum tables was substituted for the calculated momentum. Stopping pions are readily distinguished from protons by their decay.

At the time of measurement a positive print of one view of the event was taken to aid in the latter interpretation. This was useful in determining the general visible features of the event, especially the ionization and curvature of each track.

E. Spatial Reconstruction

The function of the spatial analysis program was to reconstruct the event in a three-dimensional coordinate system from measurements made in three-plane projections. The program used to process the events being reported here was developed by many people in the Walker-Erwin group at Wisconsin, principally A. R. Erwin.

F. Analysis Program

An adaptation by Leipuner and Boyd of the "Guts"[8] kinematic fitting subroutine forms the basis of the analysis program.

An attempt is made to fit each of the final states listed in reactions 1, 2, and 3; the first being a four-constraint and the latter two, one-constraint fits. In attempting to fit the first two reactions, both positive tracks are taken separately as the possible proton. This gives a total of five possible fits. The usual statistical χ^2 is calculated as a measure of goodness of fit and minimized by adjusting the measured angles and momenta within their errors subject to the over-all conditions of energy and momentum conservation.

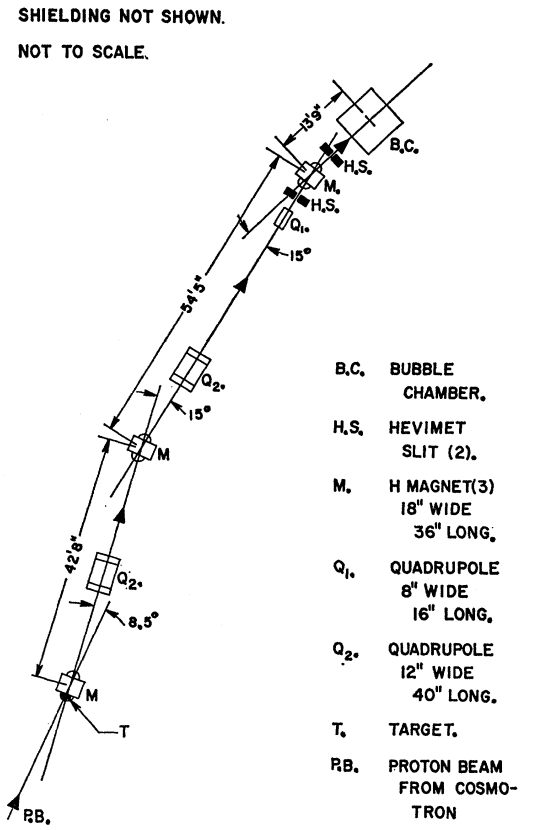

FIG. 2. Beam layout used at the cosmotron.

G. Interpretation of the Event

The determination of that positive track which may be a proton is of primary importance in the interpretation of each event. In order to do this, the ionization and range must be carefully investigated. If the momentum of the track is greater than 1 BeV/c there is no simple way of telling whether it is a proton or pion aside from gap counting. In the momentum range from 1 to 300 MeV/c, the range of a track becomes the most sensitive criterion. A proton of this momentum will have a range of 15 cm. A 200 MeV/c proton has a range of only 3.5 cm. Since there is only one nucleon entering the reaction, identification of either track as a proton eliminates the other. Estimates of the ionization of a track must take into consideration the dip angle.

There exists a kinematic criteria of the maximum angle between the incident pion and emergent nucleon. This angle has been calculated by Sternheimer[10] for various multiplicities of production. At the incident energy of this experiment and for two-pion production, the maximum nucleon angle in the lab system is 70° while for three-pion production the maximum is 63°.

By these methods at least one positive track could be identified in 78% of the events reported here. In 26%

[10] R. M. Sternheimer, Phys. Rev. 93, 642 (1953).

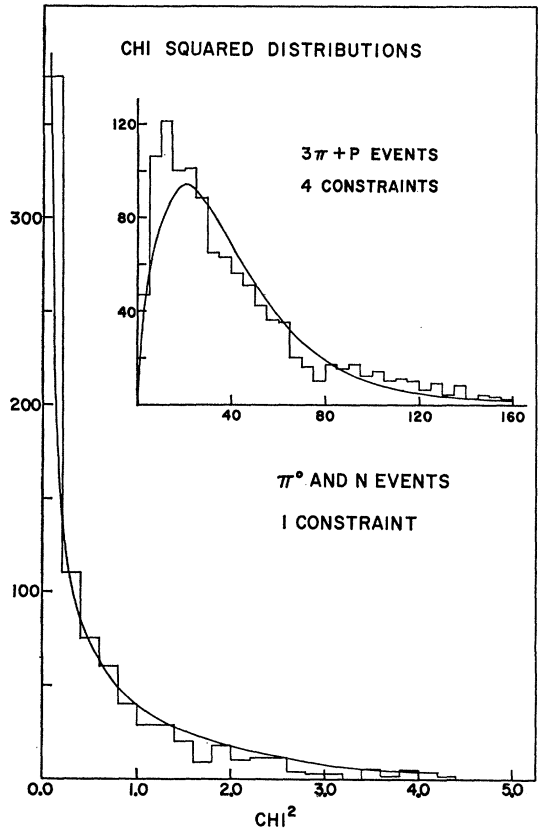

FIG. 3. Histogram of χ^2 distribution for four-prong events.

of the events one positive track could be determined to be the proton and at least one pion identified in 67% of all events. Identification of one track as a proton reduces the number of possible interpretations from five to two while identification of one pion causes a reduction to three interpretations.

Events were interpreted as reaction 1 if the χ^2 was less than 16.0 and if the track identification was consistent. Reactions 2 and 3 were considered as acceptable fits if the event had no χ^2 for reaction 1 less than 16.0 and a χ^2 for reaction 2 or 3 less than 4.0 and if the track identification was consistent. With these limits less than 5% of the one-constraint events and less than 1% of the four-constraint events would be rejected. The resulting distributions for the 4c and 1c fits are shown in Fig. 3 along with the theoretical curves. About 80% of the 4c fits had a χ^2 of less than 6.0.

Figure 4 is a histogram of the missing mass computed from the raw data of events which ultimately were classified as $\pi^+\pi^-\pi^- p\pi^0$ and $\pi^+\pi^-\pi^+\pi^- n$ final states. The arrows indicate peaks obtained for these distributions when they were plotted with Gaussian ideograms (not shown). Since these peaks occur at 139 and 945 MeV, we have some assurance that the kinematic fitting procedure is not grossly incorrect.

Ambiguous events are ones for which track identification and χ^2 limitations are not sufficient to reduce the number of possible interpretations to one. For events in this report it was possible to reduce the number of ambiguous events to 2.3% for fits to reaction 1 and to 4.8% for fits to reactions 2 and 3. Therefore, these few ambiguous events have been classified with the unambiguous ones in their respective reaction types in the following analysis.

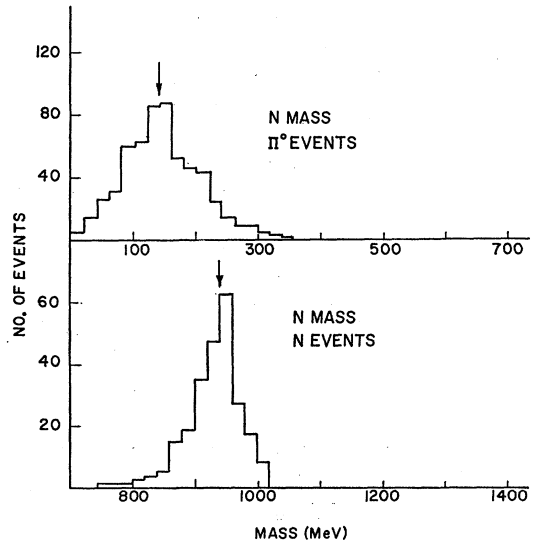

FIG. 4. Histogram of missing mass for four-prong events.

TABLE I. Mass errors and resolution functions.

	Mean error (MeV)	Full width (MeV)
4-constraint 2-body mass	5	4
4-constraint 3-body mass	10	8
1-constraint 2-body mass	8	9
1-constraint 3-body mass	17	15
1-constraint 4-body mass	20	15

H. Mass Resolution

Since a considerable part of the analysis of multiple production interactions is the study of the mass spectra of groups of emergent particles, it is very important to determine the resolution of these mass spectra.

After each fit has been obtained, the "Guts" subroutine calculates an error matrix for each track which contains the angle and momentum errors as well as the correlations between errors due to the fitting procedure. Since the constraint equations cause an interdependence of the track errors for all the tracks, the final momentum error after fitting may be reduced from the momentum error calculated in the spatial analysis program. The error in the multiparticle mass is then calculated on the basis of these fitted momentum errors. Table I presents

a summary of mean values of mass errors and widths of resolution functions for one- and four-constraint fits.

III. RESULTS

By counting the total number of interactions and, in particular, the number of four prongs in all the film used in this experiment and by using the total cross section of Longo and Moyer[11] of 35.7±0.8 mb at an incident momentum of 2.0 BeV/c, one obtains a total four-prong cross section of 3.18±0.09 mb or 1.49 μb per event. The 2128 events which have been analyzed are broken into their categories and partial cross sections in Table II.

The various mass distributions of the products of these multiple processes are compared with invariant phase-space distributions and phase-space distributions enhanced by isobar formation.

A. $3\pi+p$ Events

1. $p\pi^+$ Mass Spectrum

This mass distribution is shown in Fig. 5 with phase space normalized to all events. Each event contributes

TABLE II. Partial cross sections.

No. of events	Type	Cross section (mb)
1116	Reaction 1	1.67±0.08
577	Reaction 2	1.17±0.06
246	Reaction 3	0.37±0.02
104	Dalitz pairs	
78	Multiple, neutron and π^0	
11	Multiple, $2\pi^0$	

only once to these data. The result of formation of the 1230 MeV N_1^* state is evidently occurring for a large fraction of these events. As determined by a Gaussian ideogram (ideogram not shown), the peak lies between 1215 and 1220 MeV. To determine the number of isobar events, the phase space is normalized to the background taken to be all events above 1400 MeV. The remaining number indicates a cross section for isobar formation of 0.53±0.05 mb. The peak region can be approximately fit by a curve calculated in the following way. In the equation for the two-body phase space for a four-body final state $N_4(M_a)$, where M_a is the mass of the pion-nucleon system, the invariant two-body phase-space factor $\rho_2(M_a)$ is replaced by an analytic expression for $M_a^2\sigma_{33}(M_a)$, in which $\sigma_{33}(M_a)$ is the $\frac{3}{2}$-$\frac{3}{2}$ pion-nucleon cross section expressed as a function of the isobar mass. By this method, one assumes that the probability for forming a pion-nucleon system of mass M_a is proportional not to $\rho_2(M_a)$ but to the 3-3 scattering amplitude squared. This gives the phase space if all interactions are weighted by this

[11] M. J. Longo and B. J. Moyer, Phys. Rev. Letters 9, 466 (1962).

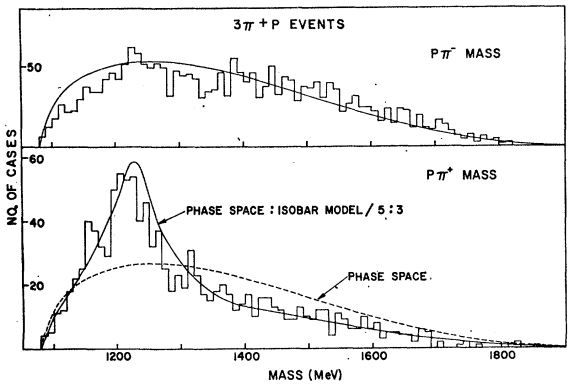

FIG. 5. Histogram of π^+-p and π^--p mass spectra for the process $\pi^-+p \to \pi^-+\pi^-+\pi^++p$.

amplitude. The area remaining after fitting the background to the usual phase space is given to this modified curve, and their sum is shown in Fig. 5. This incoherent mixing of phase space and isobar formation fits the data very well with $\frac{5}{8}$ background and $\frac{3}{8}$ isobar.

Figure 6 shows the $p\pi^+$ mass spectrum for two ranges of the angle between the incident pion and emergent proton in the over-all center-of-mass system. The mass spectrum for protons which emerge in the backward

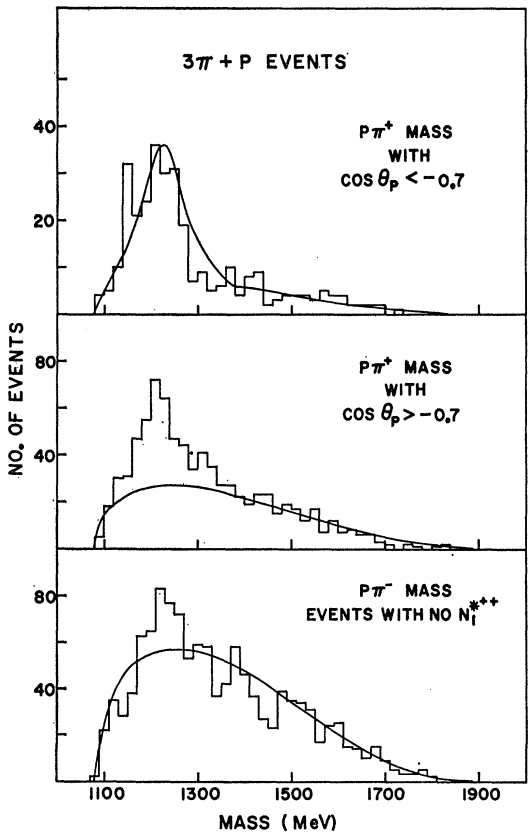

FIG. 6. Histogram of π nucleon mass spectra from events $\pi^-+p \to \pi^-+\pi^-+\pi^++p$.

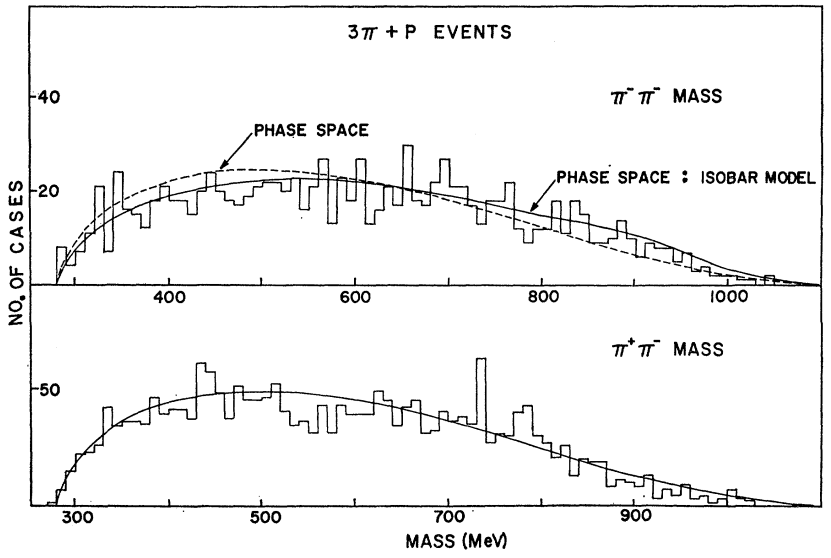

FIG. 7. Histogram of di-pion mass spectra from events $\pi^-+p \rightarrow 3\pi+p$. The solid curve is the resultant distribution from invariant phase space.

cone with $\cos\theta_p < -0.7$ shows a much higher fraction of events in the isobar peak. These data can be fit in the same manner as in Fig. 5 with now 55% of the total area accounted for by the isobar. Also shown is the spectrum for the remaining events, those with $\cos\theta_p > -0.7$. These data still clearly show evidence of isobar formation but now, of course, have a much smaller fraction of the events in the peak region. Phase space accounts for 80% of these events.

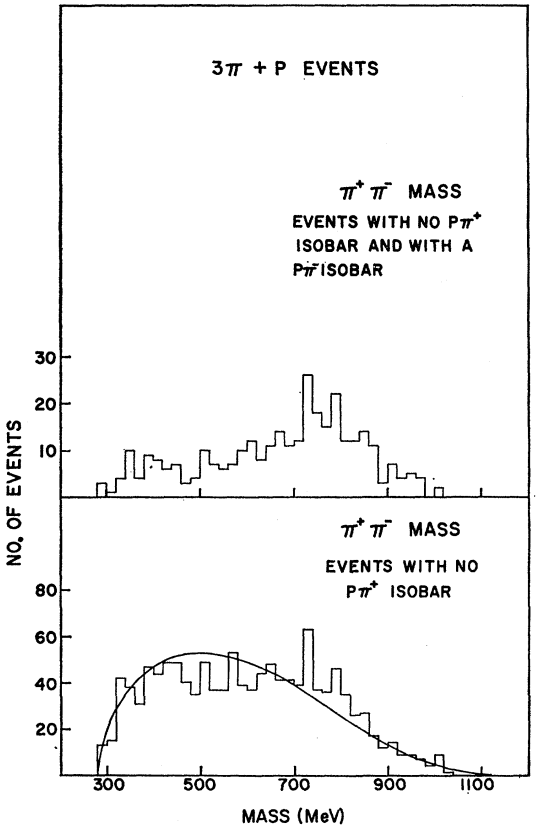

FIG. 8. Histogram of di-pion mass spectra from events without the π^+-p being in the 3,3 isobaric state.

One may note that a peak in Fig. 5 at 1150–1170 MeV, which could conceivably be a statistical fluctuation, appears more pronounced in Fig. 6 when the data are restricted to $\cos\theta_p < -0.7$. It does not appear at all for $\cos\theta_p > -0.7$. Although this peak and adjacent valley could be a fluctuation (of about 1–3% probability), this deviation occurs at a place in the mass spectrum where the production of the 1920 MeV resonance will produce an interference. This mechanism is discussed later.

2. $\pi^-\pi^-$ Mass Spectrum

The data are shown in Fig. 7 with phase space normalized to the total number of events. There do not appear to be any statistically significant peaks. The data do have a systematic shift to high $\pi^-\pi^-$ masses but this can be accounted for by the observed amount of isobar formation. Similar to the modified phase space calculated for the $p\pi^+$ mass distribution, one can calculate the effect of the 3-3 resonance on the $\pi^-\pi^-$ mass spectrum. Since the isobar mass is near the lower end of the pion-nucleon mass spectrum, the total energy in the remaining di-pion system has to be large. The curve obtained by adding $\frac{3}{8}$ of this modified phase space to $\frac{5}{8}$ of the usual phase space is also shown in Fig. 6 and fits the data somewhat better. The $\pi^-\pi^-$ mass spectrum for events with the proton in the backward cone is nearly identical to the spectrum for all events.

3. $p\pi^-$ Mass Spectrum

Figure 5 shows the mass spectrum and phase space. Each event contributes twice to these data. There is some evidence for the 3-3 isobar but the effect is small. The excess of high $p\pi^-$ masses is due to the $p\pi^+$ isobar.

In Fig. 6 these data are plotted for events without a $p\pi^+$ isobar where the latter occurs for $p\pi^+$ masses in the range from 1150–1270 MeV. The effect of the $p\pi^+$ isobar is now apparent. Considering phase space to be the background, one obtains a cross section of 0.11 ± 0.03 mb for a π^--p isobar.

4. $\pi^+\pi^-$ Mass Spectrum

These data are shown in Fig. 7 and compared to phase space. The fit is good except for the region from 700–800 MeV. At 730–740 MeV there is a sharp peak rising three standard deviations above phase space and containing 30 ± 10 events. At 770–790 MeV there is also a 2.5 standard deviation rise containing 28 ± 10 events. These maxima agree in position with the two peaks seen in the ρ^0 data of Button *et al.*[12] In order to determine if the ρ^0 is produced with an isobar, Fig. 8 shows a plot of this mass for events which do not have a $p\pi^+$ isobar. This graph also shows evidence of two ρ^0 peaks at the above-stated masses, whereas in the plot for events having a $p\pi^+$ isobar, not shown, the effect of the ρ^0 is gone. Also shown in Fig. 8 is the $\pi^+\pi^-$ mass spectrum for events which do not have a $p\pi^+$ isobar but which do have a $p\pi^-$ mass in the isobar range. This latter still clearly shows the influence of the twin peaks and indicates that ρ^0's are formed to some extent with $p\pi^-$ isobars.

The $\pi^+\pi^-$ spectrum for events with the proton in the backward cone shows the same features as the spectrum for all the data.

5. Angular Distributions

These are shown in Fig. 9. The proton and negative-pion distributions are peaked backward and forward, respectively, the proton showing more of an asymmetry. The positive pion is isotropically distributed. The angular distribution for $p\pi^+$ isobars has a higher number of events in the backward hemisphere than the proton distribution.

6. Momentum Spectra

The momentum spectra with phase-space curves are shown in Fig. 10. Also shown are the spectra predicted

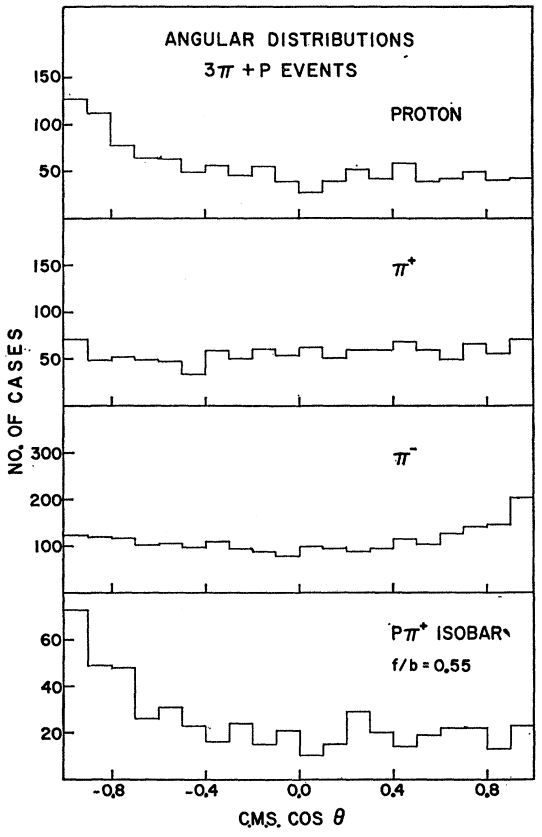

FIG. 9. Histogram of angular distributions for the various products of the reaction $\pi^-+p\rightarrow3\pi+p$.

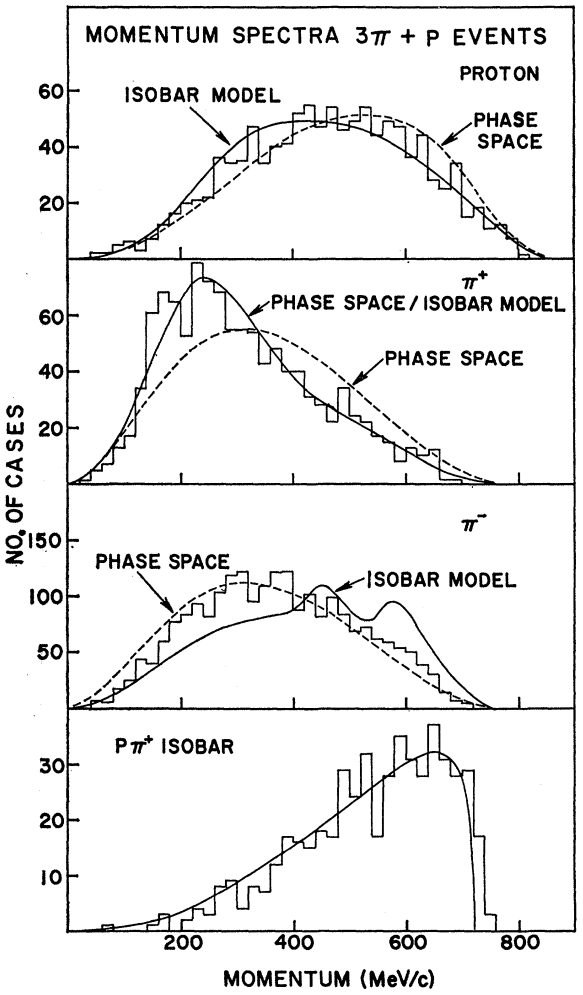

FIG. 10. Histogram of momentum spectra of products of the reaction $\pi^-+p\rightarrow3\pi+p$.

[12] J. Button, C. Kalbfleisch, G. Lynch, B. Maglic, A. H. Rosenfeld, and M. L. Stevenson, Phys. Rev. **126**, 1858 (1962).

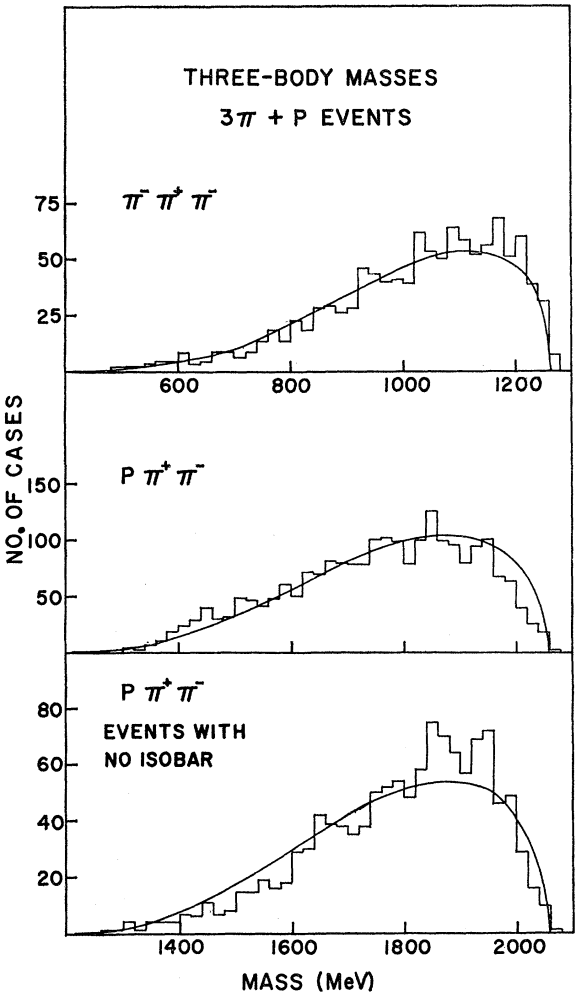

FIG. 11. Histogram of three-body mass distributions from the reaction $\pi^-+p \rightarrow 3\pi+p$.

by the Sternheimer and Lindenbaum extended isobar model.[13] For the proton, the isobar model and phase-space curves are only slightly different with the data falling between them. This agrees with the observation that the isobar is formed for somewhat less than half of the events.

The phase-space curve for the positive pion does not fit the data well due to the large excess in the 150–300 MeV/c region. The data can be fit by normalizing phase space to the data above 450 MeV/c and ascribing the remaining area to the isobar-model spectra. This fit is shown in Fig. 10. The incoherent mixing ratio is 35:65 isobar to phase space which agrees with the ratio obtained by fitting the $p\pi^+$ mass spectrum.

In the π^- spectrum there is an indication that the data are shifted to higher momenta by 50 MeV/c in comparison to phase space. There are no indications of peaks in the data corresponding to the two $T=\frac{1}{2}$ isobaric states of the pion-nucleon system.

The momentum spectrum for $p\pi^+$ isobars is shown in Fig. 10 and compared to the three-body momentum phase space for particles of mass 1230, 140, and 140 MeV. The data and phase space agree very well, indicating that isobar formation is most likely a three-body process.

7. $\pi^+\pi^-\pi^-$ Mass Spectrum

Since the final state contains only four particles, this spectrum, shown in Fig. 11, is simply related to the proton-momentum spectrum. The data are fit well by phase space showing no evidence of any $T=1$, 2, 3 resonant state.

8. Proton plus Two-Pion Mass Spectra

Because there are only four final-state particles, the $p\pi\pi$ mass spectra are simply related to the momentum spectra of the remaining pion. The $p\pi^+\pi^-$ mass dis-

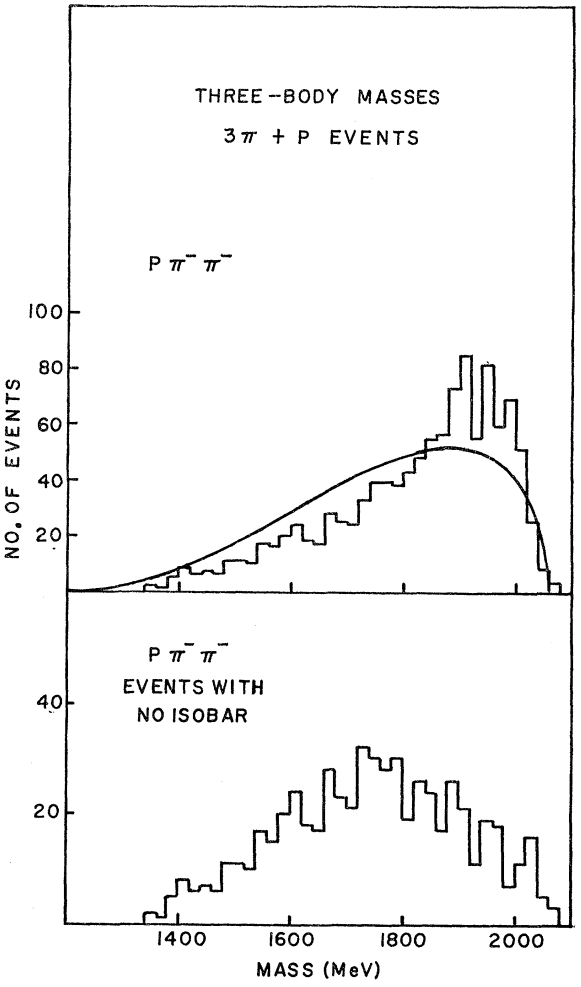

FIG. 12. Histogram of mass spectra of $p\pi^-\pi^-$ from the reaction $\pi^-+p \rightarrow 3\pi+p$.

[13] R. M. Sternheimer and S. J. Lindenbaum, Phys. Rev. 123, 333 (1961).

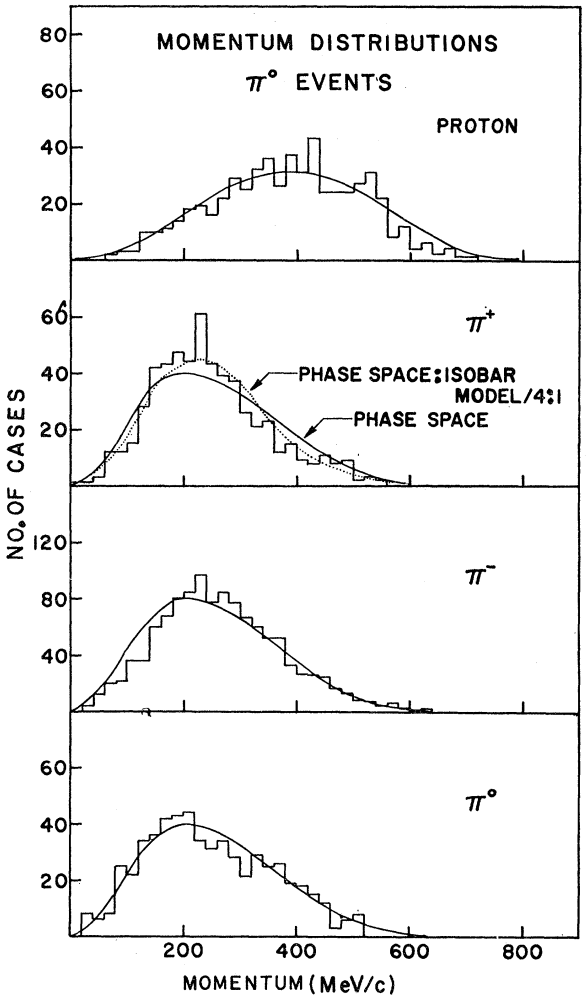

FIG. 13. Histogram of momentum spectra from products of the reactions $\pi^-+p \rightarrow \pi^-+\pi^-+\pi^++\pi^0+p$.

tribution, shown in Fig. 11, fits the phase space except for a lack of events at the high end. There is no evidence for isobaric states at 1520 or 1690 MeV. Also shown is a plot of these data omitting events which have an isobar. Now there are two peaks which draw attention, at 1840–1900 and 1920–1960 MeV. Both peaks contain about 33±16 events above a smooth curve of phase-space character. The latter peak may be some indication for the $T=\frac{3}{2}$ isobaric state at 1920 MeV which then decays directly into a nucleon and two pions.

The $p\pi^-\pi^-$ mass spectrum in Fig. 12 is expected to show the influence of the isobar already seen in the momentum spectrum. A plot of the data for events without an isobar is shown for comparison.

B. π^0 Events

A total of 571 events were acceptable as fits to the $3\pi+p+\pi^0$ final state. Using the total four-prong cross section calculated above, one obtains a π^0 cross section of 1.17±0.06 mb.

1. Momentum Distributions

The momentum spectra with their respective phase-space curves for all four types of particles are shown in Fig. 13. The proton, π^-, and π^0 data all fit phase space well, the π^- showing a slight lack of events for low momenta in the region up to 150 MeV/c. The π^+ spectrum which is most sensitive to isobar formation shows a similar structure to that seen in the $3\pi+p$ events except for extent. There is an excess in the region from 150–300 MeV/c just where the spectrum predicted for isobar decay has its maximum. In an attempt to fit this spectrum, one can assume that the momentum distribution of the decay pion from N_1^* will not be very dissimilar for this reaction compared to the $3\pi+p$ final state. The effect of the extra pion is to reduce the available center-of-mass kinetic energy. The general shape of the curve which results from adding phase space and decay spectrum is not very sensitive to the exact ratios chosen. The fit shown in Fig. 13 results from adding 15% decay spectrum to the phase space.

2. Angular Distributions

Figure 14 shows the angular distributions for particles involved in π^0 events. They are all essentially isotropic. There is no indication of any backward or forward

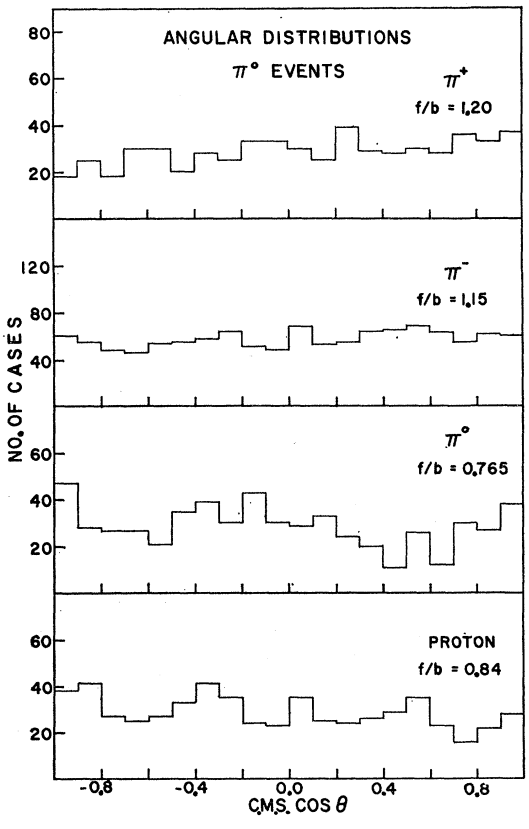

FIG. 14. Histogram of angular distributions of the products from the reaction $\pi^-+p \rightarrow 3\pi+p+\pi^0$.

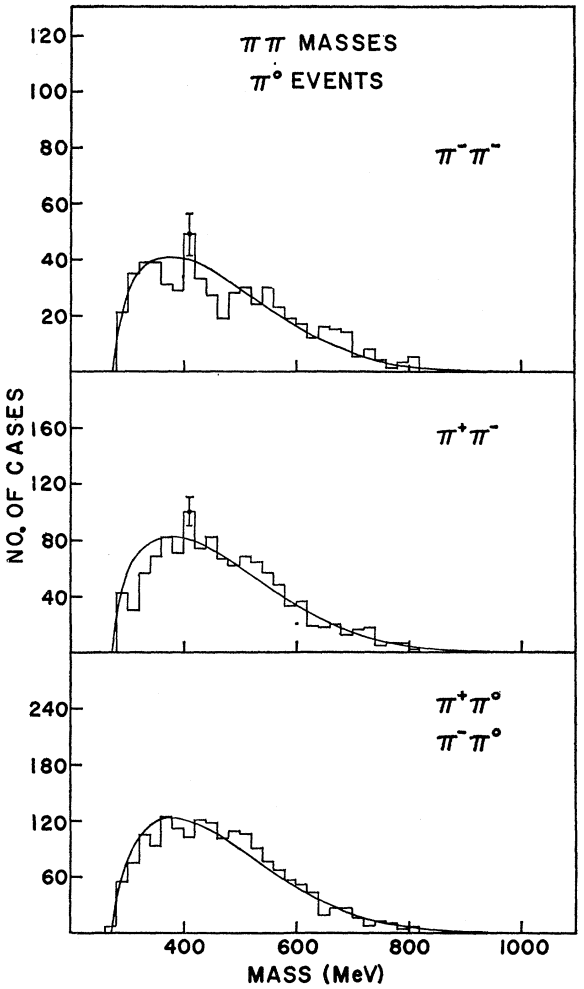

FIG. 15. Histogram of di-pion mass spectra from the reactions $\pi^-+p \rightarrow 3\pi+p+\pi^0$.

peaking of the proton or π^-, indicating that this reaction is not of a peripheral nature. The π^0 and π^+ are the most asymmetric, their forward to backward ratio being 0.76 and 1.20, respectively.

3. $\pi\pi$ Mass Spectra

In Fig. 15 are shown the mass distributions for all pairs of pions for π^0 events. The $T=2$ $\pi^-\pi^-$ spectrum if fit well by phase space. The rise at 400–420 MeV is only one standard deviation away from phase space. For the $\pi^+\pi^-$ mass, phase space also fits the data well, but again there is a slight deviation at 400–420 MeV. The $\pi^+\pi^0$ and $\pi^-\pi^0$ are shown plotted together. There is no deviation at 420 MeV as one might expect if there were some real effect.

4. Three Pion Mass Spectra

Figure 16 shows the three-pion mass-spectra and phase-space estimates for all possible charge states. Each event counts twice in the neutral 3π spectrum and once in the other two. The most striking feature is the dominance of the neutral charge-state spectrum by the η^0 and ω^0 states. The lower phase-space curve is obtained by subtracting the number of events above the total phase space in the η^0 and ω^0 peaks and normalizing to this reduced area. Considering this reduced curve as background, one obtains partial cross sections for η^0 and ω^0 production of $(0.037\pm0.015)\times3.5$ and 0.26 ± 0.035 mb, respectively. By plotting the data by means of a Gaussian ideogram program, one finds that the peaks occur at masses of 556 and 788 MeV for the η^0 and ω^0 in good agreement with the previously reported values.[4,5]

The full-width at half-maximum of the ω^0 is 35 MeV, slightly larger than the experimental resolution which has a mean value of 17.3 and a full-width of 15 MeV. The width of the η^0 peak, 20 MeV, is less significant because of the smaller number of events but is equal to the resolution.

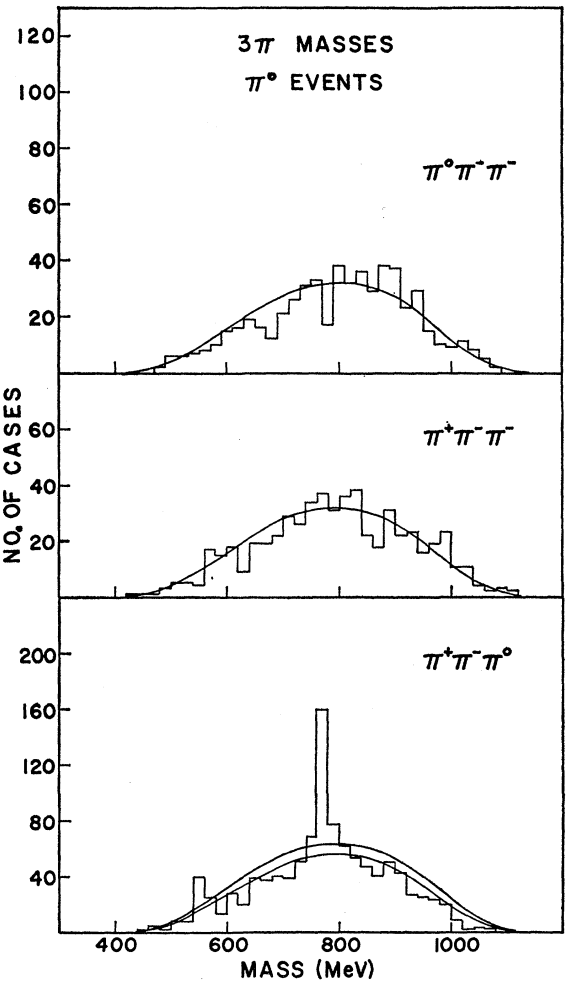

FIG. 16. Histogram of tri-pion mass spectra from the reaction $\pi^-+p \rightarrow 3\pi+p+\pi^0$.

Figure 17 shows the angular distribution and momentum spectrum for the ω^0. The mass range for ω^0's used is from 750 to 830 MeV. For events with two masses in this range both are counted. The angular distribution has only a slight excess in the forward direction. The momentum spectrum can be fit by a phase space for a three-body process for particles of mass 940, 790, and 140 MeV. Also shown in this figure is the proton-momentum spectrum and angular distribution for ω^0 events. The angular distribution shows a grouping in the backward hemisphere but there is no indication of a pole indicative of peripheral events.

The Dalitz plot for ω^0 decays, not shown, has a depopulation of events at the boundary consistent with the spin assignment of 1^{--} which has been established by Stevenson *et al.*[14] The Dalitz plot for η^0 events, shown in Fig. 18, contains 38 points of which 25 ± 10 are η^0's. Events are plotted whose 3π mass lies between 540 and 560 MeV. It is apparent that low values of the neutral pion kinetic energy are favored in agreement with previous compilations.[15,16] These distributions are only compatible with the spin assignment of 0^{-+}.

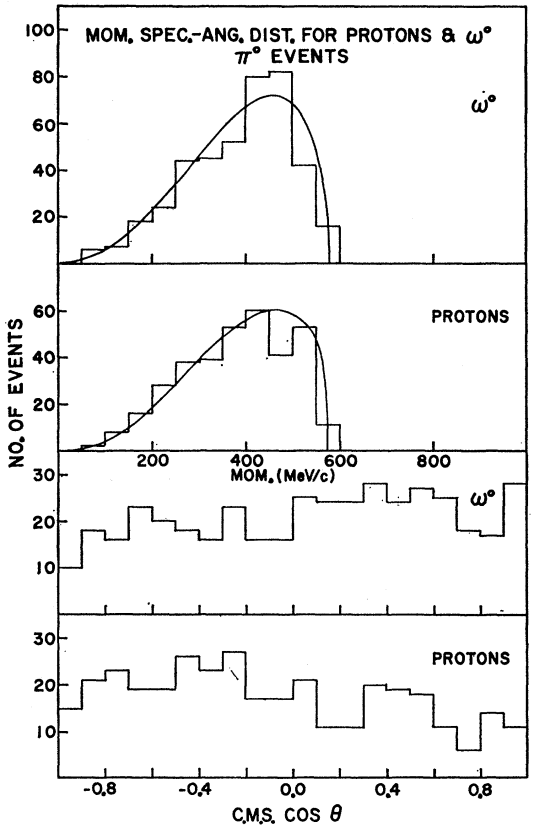

FIG. 17. Histogram of angular distributions and momentum spectra for p and ω^0 from the reactions $\pi^-+p\rightarrow 3\pi+p+\pi^0$.

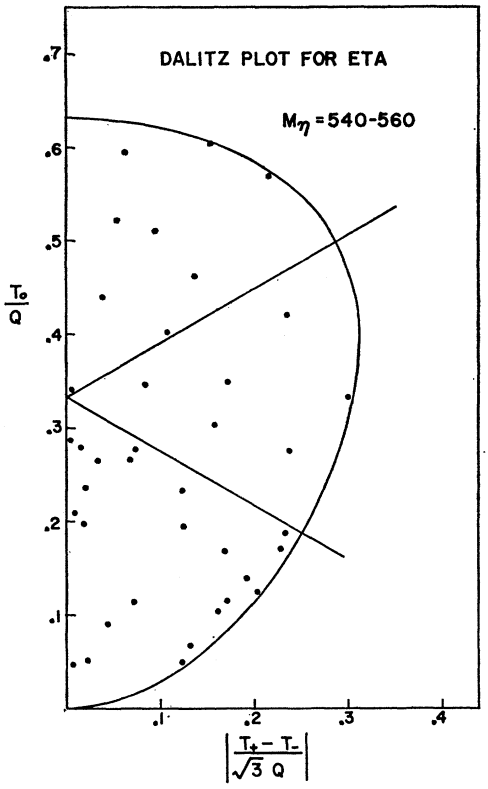

FIG. 18. Dalitz plot for the η^0's.

Figure 19 shows the mass spectra for pairs of pions for events with an omega. There are three charge states, $\pi^+\pi^0$, $\pi^-\pi^0$, and $\pi^+\pi^-$, the former two being plotted together. Since one knows the spin and parity of the omega, one can determine the matrix element and include its effect in the three-body phase-space calculation. The process is analyzed by considering the omega to break up into a di-pion and a pion followed by the decay of the di-pion. Letting the momentum of the pions from the di-pion decay be q in the di-pion rest frame and the momentum of the di-pion be p in the omega rest frame, the matrix element squared is proportional to p^2q^2, aside from a factor of $1-\mu^2$, where μ is the cosine of the angle between p and q. As seen in Fig. 19, the resulting modified phase space fits the data very well for all charge states.

Also shown in Fig. 19 are the $p\omega^0$ and $\pi^-\omega^0$ masses, with the appropriate three-body phase-space curves, assuming the final state to consist of a proton, a pion, and an omega.

The $\pi^{0,+}\pi^-\pi^-$ mass data, also shown in Fig. 16, do not appear to exhibit any disagreement with phase space.

[14] M. L. Stevenson, L. W. Alvarez, B. C. Maglic, and A. H. Rosenfeld, Phys. Rev. **125**, 687 (1962).

[15] C. Alff, D. Berles, D. Colley, N. Gelfand, U. Nauenberg, D. Miller, J. Schultz, J. Steinberger, T. H. Tan, H. Brugger, P. Kramer, and R. Plano, Phys. Rev. Letters **9**, 322 (1962).

[16] P. L. Bastien, J. P. Berge, O. I. Dahl, M. Ferro-Luzzi, D. H. Miller, J. J. Murray, A. H. Rosenfeld, M. B. Watson, Phys. Rev. Letters **8**, 114 (1962).

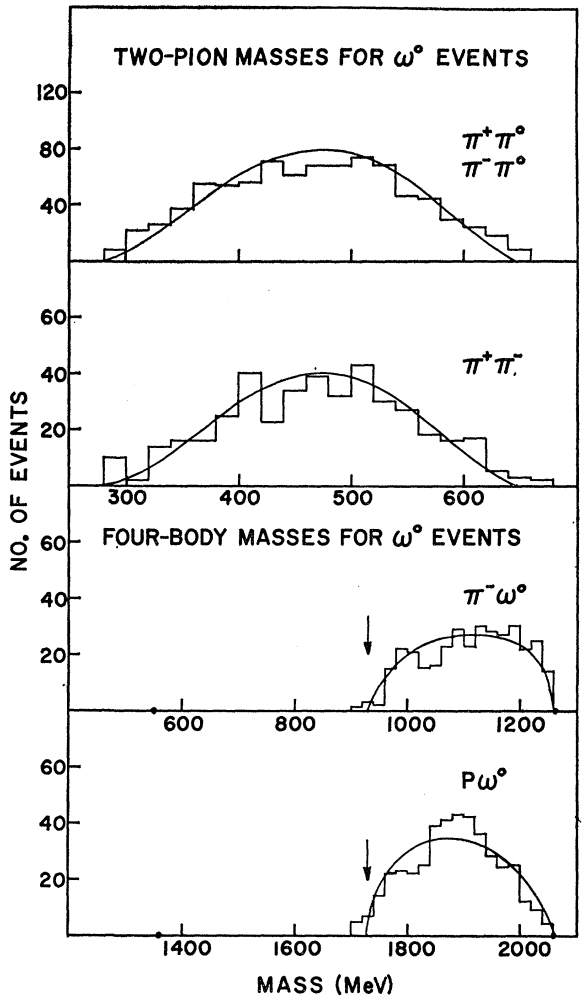

FIG. 19. Histogram of di-pion mass spectra for di-pions coming from the decay of ω^0. Also, $\pi^-+\omega^0$ and $p+\omega^0$ mass spectra from events $\pi^-+p \rightarrow \omega^0+\pi^-+p$.

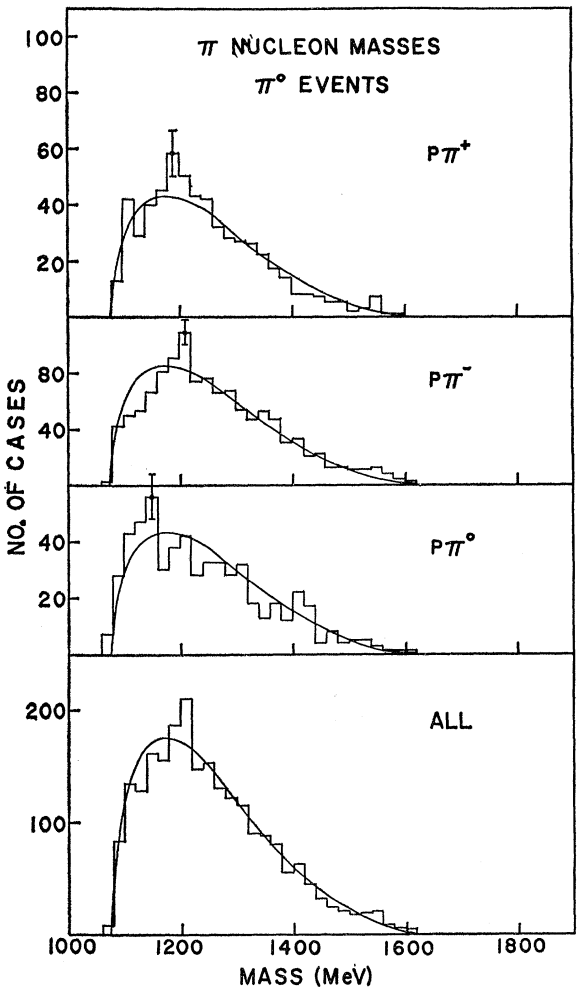

FIG. 20. Histogram of π nucleon mass spectra from the reaction $\pi^-+p \rightarrow 3\pi+p+\pi^0$.

5. *Pion-Nucleon Mass Spectra*

These spectra are compared to phase space in Fig. 20. There are three possible charge states, $p\pi^+$, $p\pi^0$, and $p\pi^-$, each event contributing once to the first two states and twice to the last. The last graph in Fig. 20 shows the spectrum for all the data combined. It is immediately apparent that the N_1^* state is not a dominant effect in these data. The $p\pi^+$ and $p\pi^-$ do show an excess in the isobar region but the $p\pi^0$ does not. The peaks occur somewhat lower than the nominal 1230 MeV due to the effect of phase space which has its maximum at 1170 MeV. The cross sections are 57 ± 22 and 24 ± 21 μb for the $p\pi^+$ and $p\pi^-$ isobars, respectively.

Since the production of an ω^0 is important for these events, it is of interest to observe the pion-nucleon mass spectra for events with and events without an ω^0. The data are shown in Fig. 21. The $p\pi^+$ isobar is most apparent for events wherein an ω^0 is not formed. The last graph in Fig. 21 seems to show evidence that the $p\pi^-$ isobar occurs more frequently when an ω^0 is produced. However, when one counts the number of events which contribute twice to the peak, the number of counts above phase space is reduced to 18 ± 12. The fact that there is little π^+-p isobar production in ω^0 events is not surprising since the ω^0 is probably long lived and the π^+ has a relatively small chance to rescatter from the proton.

6. *Nucleon and Two-Pion Mass Spectra*

These spectra for all charge combinations are compared with phase space in Fig. 22. There does not appear to be any significant deviation in any of the data. In particular, there is no indication of formation of the 1520 or 1690 MeV isobaric states.

7. *Four-Body Mass Spectra*

Figure 23 gives the mass spectra for all combinations of four-body states. It is evident that the data are well

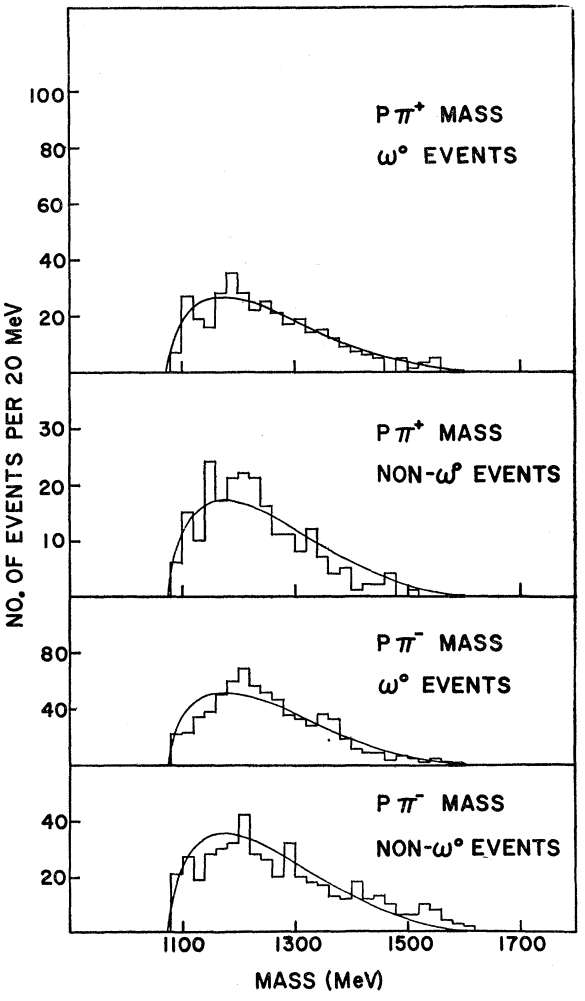

FIG. 21. Histogram of π—nucleon mass spectra from the reaction $\pi^-+p \rightarrow \omega^0+\pi^-+p$ and others.

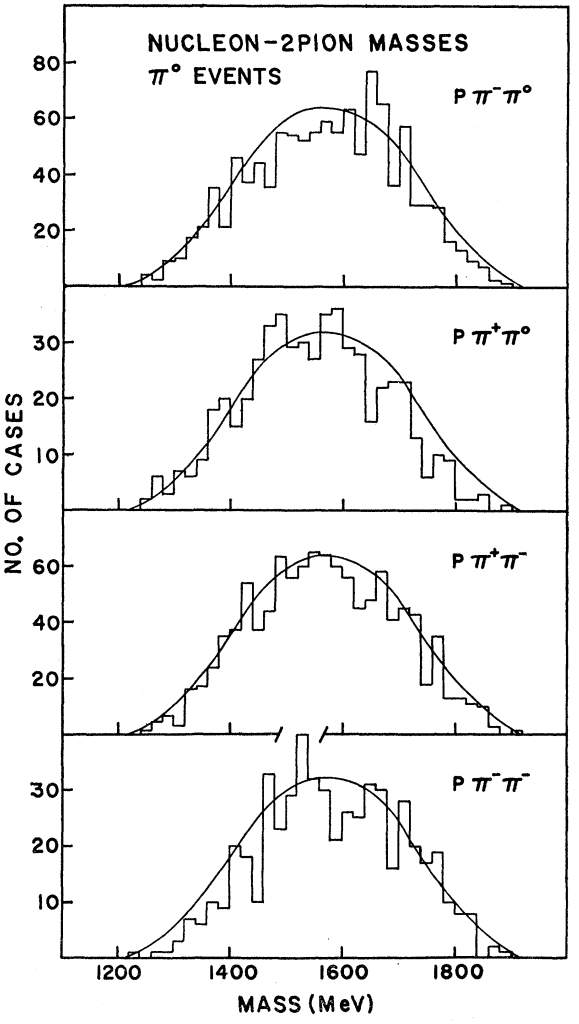

FIG. 22. Histogram of mass spectra of nucleon-di-pion combinations from events $\pi^-+p \rightarrow 3\pi+p+\pi^0$.

accounted for by phase space, except possibly for the $p\pi^0\pi^-\pi^-$ spectrum. Since the final state contains five particles, these data are a kinematic consequence of the π^+ momentum spectrum which, as noted above, gives some evidence of isobar formation. The range of excess in the mass distribution is 1890–2010 MeV which is equivalent to a range in the π^+ momentum of 275–185 MeV/c. This is just where the momentum excess occurs. Since this mass combination may have $T_3=\frac{3}{2}$, there may be also some effect of the 1920-MeV nucleon excited state, but the amount is difficult to determine.

C. Neutron Events

A total of 246 events was found to fit reaction 3 giving a total cross section of 0.37 ± 0.02 mb. The details of these events are discussed in the following sections.

1. *Angular Distributions for n Events*

Figure 24 shows the angular distributions for the π^-, π^+, and n. Both pions are distributed with a slight excess in the forward hemisphere. The forward excess of the π^- occurs in the cone with $\cos\theta>+0.7$, whereas the excess of π^+ is due to a general lack of events in the backward hemisphere. The neutron distribution is peaked backward.

2. *Momentum Spectra for n Events*

The momentum-spectra and phase-space curves are shown in Fig. 25. For the neutron and π^+ the agreement is good. The π^-, however, shows a deviation in the region from 180–280 MeV/c which seems to indicate that the N_1* isobar is being formed for some fraction of these events. The $n\pi^-$ is a pure $T=\frac{3}{2}$ state. This peak agrees in position with that expected from decay of the

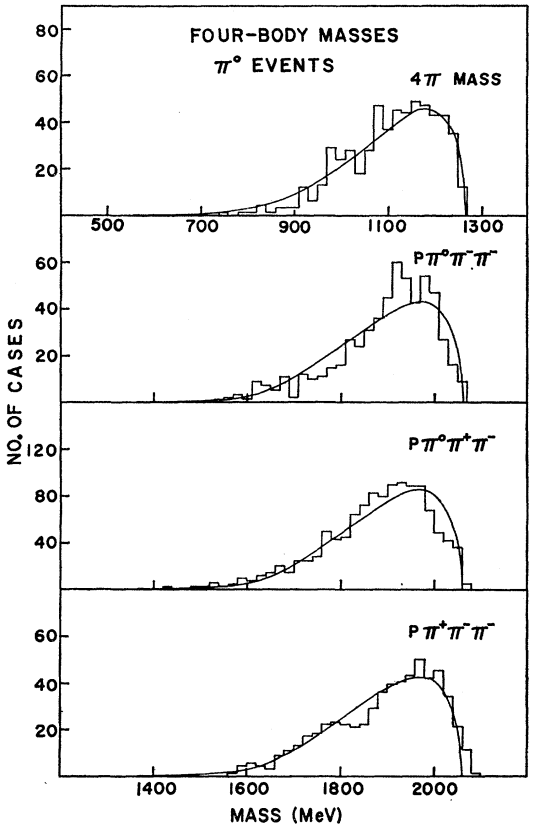

FIG. 23. Histogram of four-body mass spectra from the reaction $\pi^-+p \rightarrow 3\pi+p+\pi^0$.

N_1* into a neutron and π^-. Because of the small amount of deviation from phase space it is difficult to estimate the fraction of events in the peak by trying to fit the momentum spectrum.

3. *Two-Body Masses*

In Fig. 26 are shown the plots of all possible two-body systems for neutron events. The $\pi^+\pi^+$ and $\pi^-\pi^-$ are plotted together since they must be in a pure $T=2$ isotopic spin state. There are four combinations of $\pi^+\pi^-$ and two of $n\pi^+$ and $n\pi^-$ for each event. The only spectrum which shows any deviation from phase space is that for the $n\pi^-$ which is where one expects to see the effect, if any, of the isobar. To determine the cross section, one must count the number of events above phase space and subtract those which contribute twice to the peak. The result is 0.018 ± 0.016 mb.

4. *Three-Body Masses*

There are four combinations of three-body states which can be observed. These are shown in Fig. 27. Each event contributes four times to the 3π and $n\pi^+\pi^-$ masses and once each to the $n\pi^+\pi^+$ and $n\pi^-\pi^-$. The three-pion masses are plotted together since their isotopic spin states must be the same. There are no indications of any deviations from phase space.

5. *Four-Body Masses*

The three combinations of four-body masses are shown in Fig. 28. Each event contributes twice to each neutron-three-pion mass and once to the four-pion mass. The four-pion and $n\pi^+\pi^-\pi^-$ masses do not deviate from phase space. The $n\pi^+\pi^+\pi^-$ does but in a manner which can be understood, at least in part, by the amount of isobar formation. This is the same situation as in the $p\pi^-\pi^-\pi^0$ mass for π^0 events. The mass excess may be a consequence of the deviation in the π^- momentum spectrum which, as seen before, also has a peak region. The excess in the mass distribution from 1850–2010 MeV, which is equivalent to a momentum range from 270–185 MeV/c, contains the same number of events as the excess in the momentum distribution. If the 1920-MeV nucleon excited state is contributing to this part of the mass spectra, interference with $n\pi^-$ isobar formation makes a simple separation of the two effects difficult.

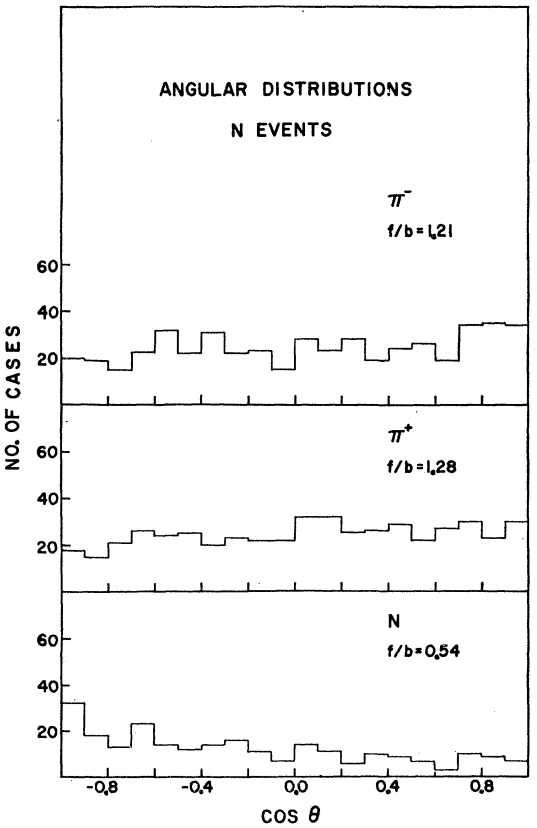

FIG. 24. Histogram of angular distributions of products from the reaction $\pi^-+p \rightarrow 2\pi^-+2\pi^++n$.

IV. CONCLUSIONS

In general most of the distributions found in this experiment are describable in terms of a phase-space distribution. This means that one particular diagram does not dominate the process. One can hope by various separation methods to isolate the effect of particular diagrams but with the realization that interference will still certainly be present in a consequential fashion.

A. $3\pi+p$ Events

The production of the N_1^* isobar is an important process in the $3\pi+p$ final state. The fits to the $p\pi^+$ mass spectrum and also the π^+ momentum spectrum determine that $37\pm5\%$ of these events proceed by means of the isobar production. The diagram for this process may be the following shown in Fig. 29.

Production of isobars is favored for low-momentum transfers as indicated by Fig. 30, which shows the square of the four-momentum transfer Δ^2 to the $p\pi^+$ isobar. These data are in agreement with the prediction of Salzman and Salzman[17] that the spectra should be proportional to the propagator $1/(\Delta^2+\mu^2)^2$ corrected for the off-the-mass-shell pion by the factor $(W-M)^2+\Delta^2$ where W is the isobar mass, M the proton mass, and μ the pion mass. The fit is good up to momentum transfers of 70–80 in units of Δ^2/μ^2; the apparent deviation for low Δ is a kinematic effect. Above this point the data agree with the Δ^2 spectrum calculated by assuming the isobar-momentum spectrum to be derived from the three-body phase space for a system composed of two pions and an isobar with an isotropic distribution. For events where there is no $p\pi^+$ isobar, Fig. 31 shows that the momentum transfer to the proton agrees quite well with the spectrum calculated assuming the proton-momentum spectrum to be de-

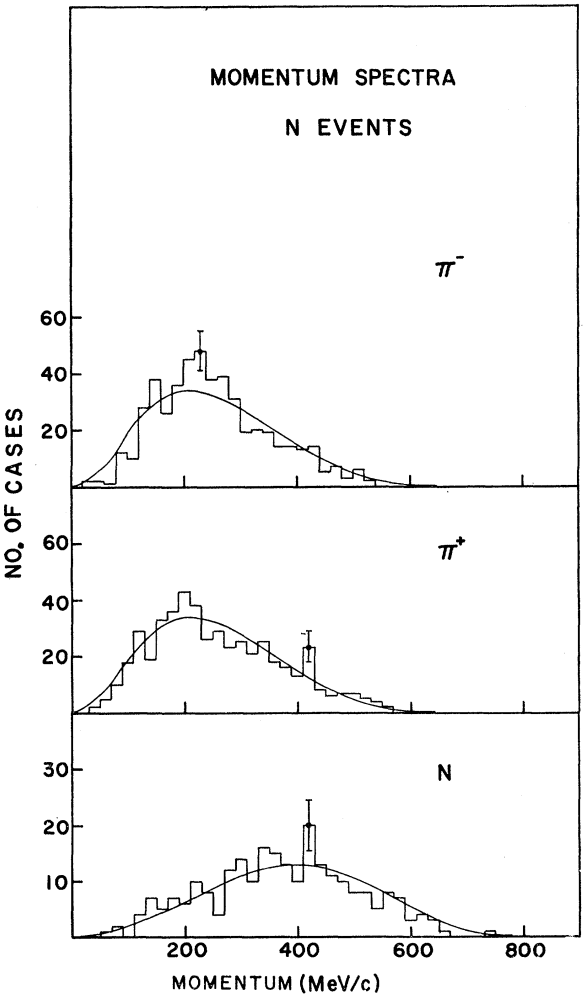

FIG. 25. Histogram of momentum spectra of products from the reaction $\pi^-+p\rightarrow 2\pi^-+2\pi^++n$.

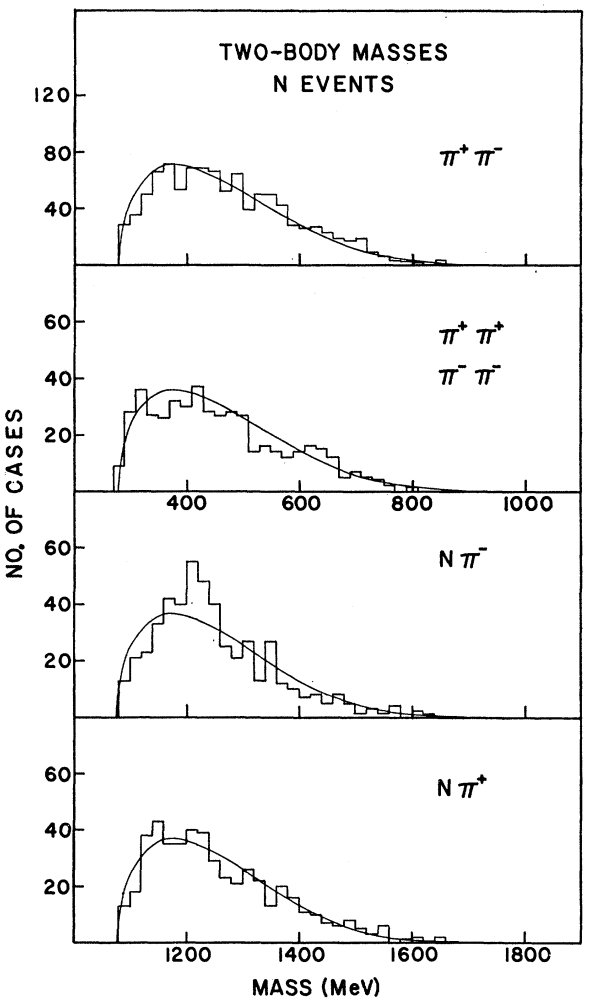

FIG. 26. Histogram of two-body mass spectra from the reaction $\pi^-+p\rightarrow 2\pi^-+2\pi^++n$.

[17] F. Salzman and G. Salzman, Phys. Rev. **120**, 599 (1960).

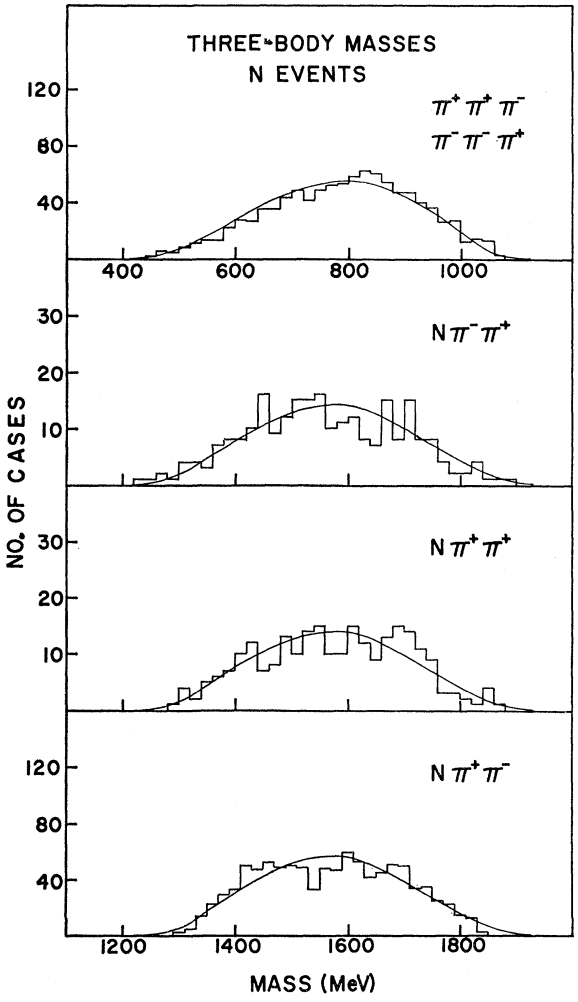

FIG. 27. Histogram of three-body mass spectra from the reaction $\pi^-+p \rightarrow 2\pi^-+2\pi^++n$.

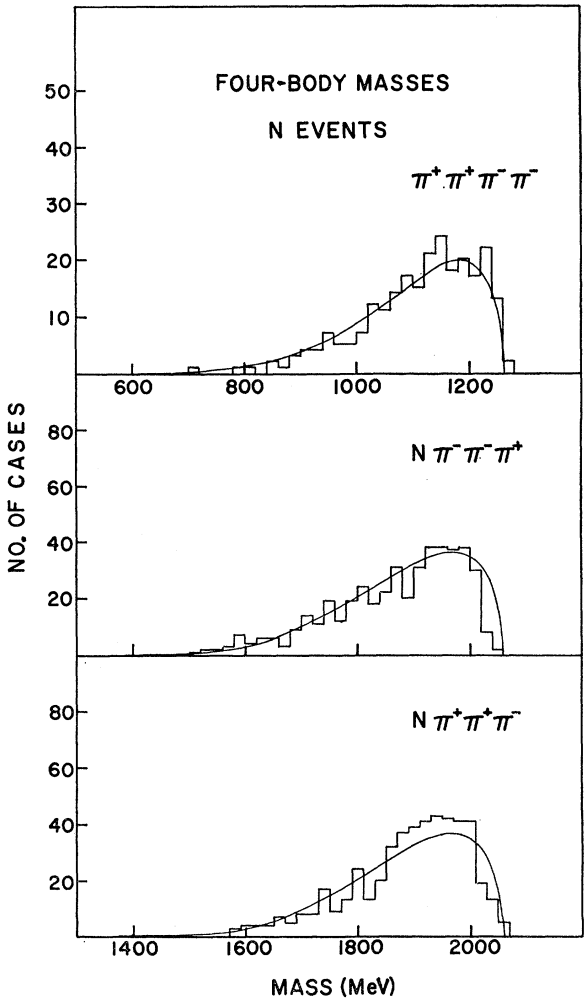

FIG. 28. Histogram of four-body mass spectra from the reaction $\pi^-+p \rightarrow 2\pi^-+2\pi^++n$.

rived from the four-body phase-space factor for a system of three pions and a proton. The angular distribution of isobars which is peaked 2:1 in the backward direction also shows that low-momentum transfers are favored for isobar production.

If the above diagram is assumed to represent isobar events, one can calculate a $\pi^-\pi^-$ cross section at the upper vertex following the method described by Salzman and Salzman.[17] They show that for sufficiently small values of Δ^2, the square of the four-momentum transfer to the isobar, the virtual pion behaves as an almost real particle at both vertices with the result that the $3\pi+p$ cross section would be given by

$$\frac{\partial^3\sigma}{\partial(\Delta^2)\partial(W^2)\partial(V^2)}=\frac{1}{2(2\pi)^3 k_{iL}{}^2M^2}\times\frac{\sigma_{\pi\pi}(V_1\Delta^2)k_V V\sigma_{\pi N}(W_1\Delta^2)k_{3W}W}{(\Delta^2+\mu^2)^2}$$

where the following quantities are used:

(1) W = the total energy in the isobar rest system,
(2) V = the total energy in the di-pion rest system,
(3) k_V = momentum of pions in the di-pion system,
(4) k_{3W} = momentum of pion in isobar rest system,
(5) k_{iL} = momentum of incident pion in lab system,
(6) M = mass of proton,
(7) μ = mass of pion.

Using this formula "as is" to deduce a π-π cross section is probably not a very reliable method. Salzman and Salzman[17] and others have tried to deduce "off-the-mass-shell" corrections. To date none of the formulas seem to give reliable results. The difficulty probably has to do with interference from other diagrams. A correction of some sort would not very naturally be in terms of a more or less universal multiplicative cor-

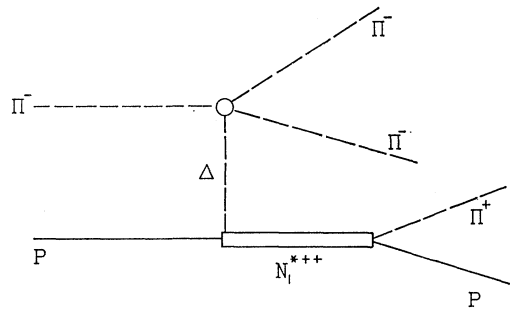

FIG. 29. A possible diagram for the production of $3\pi+p$ final states by one-pion exchange in π^-+p collisions.

section factor. Our results on single-pion production reem to give correct answers within a factor of two.

We integrate the cross-section formula omitting any corrections. The results of this calculation are shown in Fig. 32 where the maximum momentum transfer allowed is 600 MeV/c. The results show a roughly constant cross section of about 30 mb. A better knowledge of the momentum transfer dependence of the partial cross section at the pion-nucleon vertex would give a better approximation.

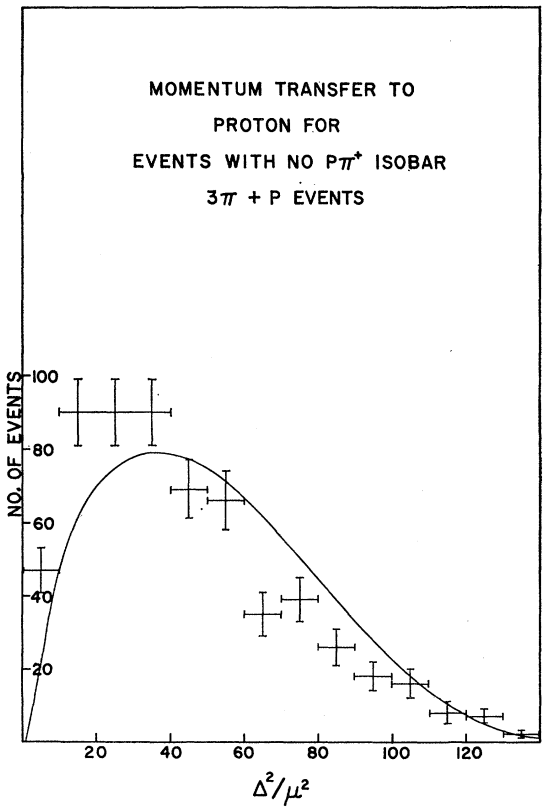

FIG. 30. Spectrum of momentum transfers to the $\pi^+ + p$ isobar in events of $\pi^- + p \rightarrow 3\pi + p$. The solid curve is a theoretical curve of $[(W-M)^2+\Delta^2]/(\Delta^2+\mu^2)^2$ without putting in effects of kinematic cutoff.

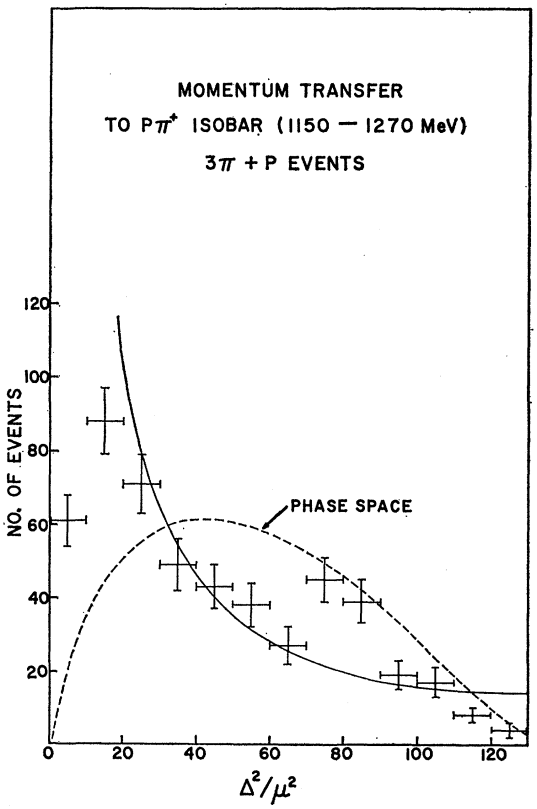

FIG. 31. Spectrum of momentum transfers to the proton for events of the type $\pi^- + p \rightarrow 3\pi + p$ with no $\pi^+ - p$ isobar. The dashed curve is calculated assuming that the proton-momentum spectrum is governed by phase space and that the protons are isotropically distributed.

Since there is evidence in these events for the excitation of the $p\pi^+$ and also the $p\pi^-$ isobaric states in peripheral collisions, it is possible to use the ratio of the cross sections for these processes to draw some tentative conclusions about the π-π scattering cross sections. Consider the two diagrams in Figs. 29 and 33. The cross sections for $p\pi^+$ and $p\pi^-$ isobar production

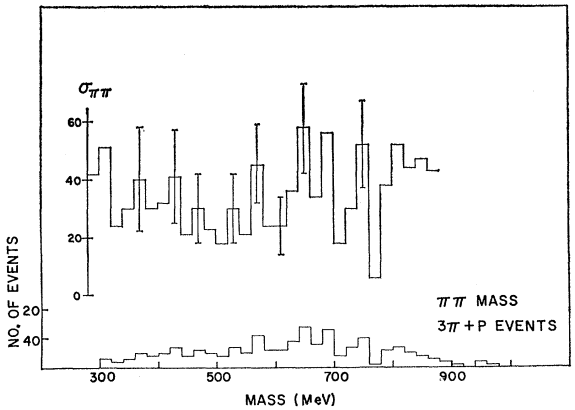

FIG. 32. Histogram of $\pi^- - \pi^-$ cross section calculated from events $\pi^- + p \rightarrow 3\pi + p$ assuming the peripheral model.

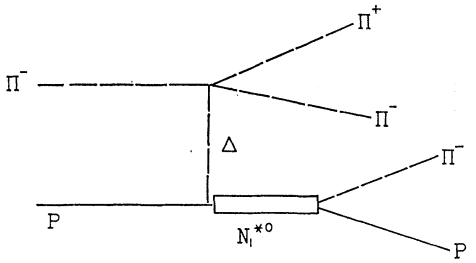

FIG. 33. A possible diagram for the production of $3\pi+p$ final states by one-pion exchange in π^-+p collisions.

are 0.53±0.05 and 0.11±0.03 mb, respectively. In Fig. 29 the π-π vertex must be a pure $T=2$ state, while in Fig. 33 it is a mixture of $T=0$, 1, and 2. The $\pi^+\pi^-$ isotopic spin function is

$$|\pi^+\pi^-\rangle=(\tfrac{1}{6})^{1/2}|2,0\rangle+(\tfrac{1}{2})^{1/2}|1,0\rangle+(\tfrac{1}{3})^{1/2}|0,0\rangle.$$

We use the known cross sections for π^-+p and π^++p in the region of the "3,3" isobar and assume that essentially only S-wave π-π scattering occurs at the upper vertex. The peripheral model then gives us the ratio of $I=0$ to $I=2$ π-π cross section over a range of 300 to 600 MeV. The result is $\sigma_0/\sigma_2=5\pm2$.

Since there is some evidence that ρ^0 and $p\pi^-$ isobar are produced together, the diagram in Fig. 33 might be contributing to these events. The $\pi^+\pi^-$ mass spectrum has a double peak with cross sections $\rho_1{}^0=45\pm15$ μb and $\rho_2{}^0=42\pm18$ μb. This double peak effect is also seen in the neutron π^+ and π^- two-prong data from this

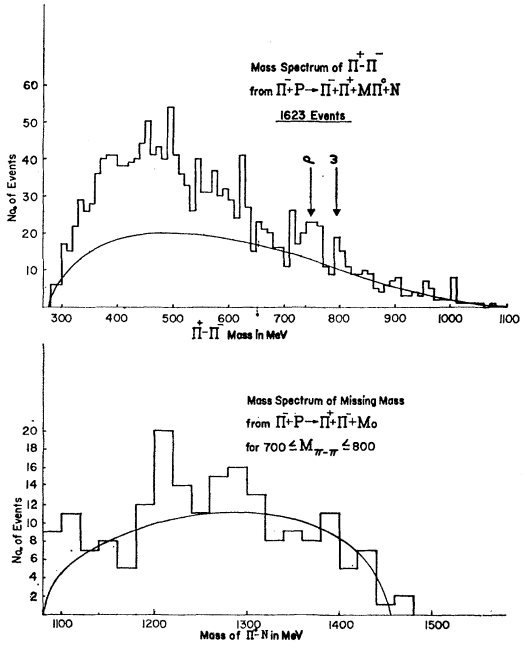

FIG. 34. Histogram of mass spectra from events of the type $\pi^-+p\rightarrow\pi^-+\pi^0+m\pi^0+n$.

experiment.[18] There is also evidence from other experiments that the ρ^0 and isobar final states are important. Samios *et al.*[19] noted considerable effect of the ρ^0 in the $\pi^+\pi^-$ mass spectrum for data obtained at a π^- beam momentum of 4.7 BeV/c. Carmony *et al.*[20] have presented data at an incident momentum of 2.03 BeV/c which is very similar to that shown here. They find that 27±3% of the $3\pi+p$ events have a N_1* isobar and that this process is favored for low-momentum transfers. Alff *et al.*[15] in $p\pi^+$ interactions at 2.34, 2.62, and 2.90 BeV/c also find that $3\pi+p$ events are dominated by the isobar with the $\pi^+\pi^-$ coming from the decay of a ρ^0. Since the initial state is doubly charged, it is possible to produce a 3,3 $p\pi^+$ isobar and a ρ^0.

In Fig. 34 we show the $\pi^+\pi^-$ mass distribution from events of the type $\pi^-+p\rightarrow\pi^-+\pi^++m\pi^0+n$ where m is probably 1 or 2. A large fraction of these events are consistent with being events of the type $\pi^-+p\rightarrow\omega^0+n$ and $\pi^-+p\rightarrow\omega+\pi^0+n$ in that the di-pion mass spectrum shows a large peak in the 400–500-MeV mass range as expected from the decay of the ω^0. We notice also that there are peaks in the 700–800-MeV region, the first peak being consistent with ρ^0 production and the second from the 2π decay of the ω^0. The ρ^0 appears to be much broader in the process $\pi^-+p\rightarrow\rho^0+\pi^0+n$ than in the process $\pi^-+p\rightarrow\rho^0+\pi^-+p$. This can be construed as the effect of interference with some other process giving rise to 3 pions and a nucleon. If the peripheral diagram with 3,3 production dominated the production of $\rho^0+\pi+$nucleon, then we would except the products $\rho^0+\pi^0+n$ to be twice as numerous as $\rho^0+\pi^-+p$. In fact they are about 5 to 10 times as numerous which shows that the pion-exchange diagram does not dominate this latter process. In Table III we give a resumé of cross sections for $\rho^0+N^{*0}(\pi^-+p)$, $\rho^0+N^{*0}(\pi^0+n)$, $\rho^0N^{*++}(\pi^++p)$ at this energy. The data on π^++p have been taken from recent results of James and Kraybill.[21]

B. π^0 Events

The most apparent effect in this event class is the production of the ω^0. One finds that 29.5±4.0% of these events have an ω^0 in the final state. The ω^0 is produced isotropically indicating that the production mechanism is not peripheral. This is further illustrated by comparing the spectrum of the momentum transfer to the proton for events with an ω^0 to that for all the events combined. Figure 35 shows that these two distributions are the same. The data are shown com-

[18] W. D. Walker, University of Wisconsin (unpublished data).
[19] N. P. Samios, A. H. Bachman, R. M. Lea, T. E. Kalogeropoulos, and W. D. Shephard, Phys. Rev. Letters **9**, 139 (1962).
[20] D. D. Carmony, F. Grard, R. T. Van de Walle, and N. Xuong, in *Proceedings of the 1962 Annual International Conference on High-Energy Physics at CERN*, edited by J. Prentki (CERN, Geneva, 1962), 44.
[21] Frederick E. James, H. L. Kraybill (to be published). We thank the authors for sending us their results prior to publication.

TABLE III. Comparison of ρ, ω, η. Production by $\pi^+ + p$ and $\pi^- + p$ at 2.1 Bev/c.

	$\pi^-+p+\rho^0$	$\pi^0+n+\rho^0$	$\pi^+ + p + \rho^0$	$\pi^- + p + \omega^0$	$\pi^+ + p + \omega^0$	$\pi^- + p + \eta^0$	$\pi^+ + p + \eta^0$
σ in mb	0.045±0.15	0.227±0.06	1.5±0.2	0.26±0.035	1.6±0.2	0.15±0.06	0.6±0.2

pared with the prediction of the one-pion exchange model[17] $\Delta^2/(\Delta^2+\mu^2)^2$ and a calculation of the distribution expected from the known momentum phase space of the proton. Both types of data points follow the phase-space calculation very well.

The work of Carmony *et al.*[20] indicated that the production cross section was 0.142±0.031 mb, while for this experiment it is found to be 0.26±0.035 mb. This increase is quite large when one considers that it occurs for an increase in the beam momentum of only 70 MeV/c. Diddens *et al.*[22] have recently shown that there is a rapid rise in the $\pi^- p$ total cross section at a kinetic energy of 2.0 BeV. The cross section increases from 33.7 mb at a kinetic energy of 1.6 BeV to 35.4 mb at 2.0 BeV followed by a decrease to 33.6 mb at 2.3 BeV. The change in the production may account in part for this rapid change in the total cross section.

Alff *et al.*[15] found that a large fraction of the ω^0's produced in the reaction $\pi^+ + p \to \pi^+ + p + \omega^0$ were associated with the production of the $\pi^+ + p$ in the 3,3 resonance. We summarize our data on ω^0 production and the data of James and Kraybill[21] which were obtained using $\pi^+ + p$ at a momenta of 2.08 BeV/c in Table III. Using the usual arguments involving Clebsch-Gordan coefficients and the fact that the ω^0 has isotopic spin 0 we expect the ratio of π^+ to π^- cross section to be 9:1 if the production goes via $T=\frac{3}{2}$ isobar production. We find a ratio 6±1 which shows a dominance of the $T=\frac{3}{2}$ with some admixture of $T=\frac{1}{2}$ for the $\pi^- p$ combination.

The attempt to observe the isobar directly by looking at a proton-pion mass spectra for events with an ω^0 does not give a strong indication of isobar formation. This method is not very sensitive, however, since phase space has its rather broad maximum just where the isobar peak would be. As a result, the estimation of effect and background becomes very subjective. One can only conclude that there is some evidence here for the formation of an isobar and ω^0 final state. The main evidence for isobar dominance comes from the branching ratio of π^+ and π^- production.

The two-pion mass spectra for ω^0 decays do not show any evidence that the decay mode $\omega \to \xi + \pi$ is contributing. Feinberg[23] has shown that this decay mode would be dominant if the ξ existed. Also, the effect of the ξ would be seen in a band structure of the ω^0 Dalitz plot. Since neither of these effects is seen, the existence of the ξ is dubious. If the ξ does not exist, Feinberg and Bernstein[24] and Glashow[25] show that the two-pion decay mode of the ω^0 may contribute a second peak in the neutral ρ mass spectrum. If the upper peak in the neutral two-pion mass spectrum for $3\pi+p$ events is due to this decay mode, then the branching ratio of charged two pion to charged two pion and charged three pion is

$$\frac{\omega \to \pi^+ + \pi^-}{(\omega \to \pi^+ + \pi^-) + (\omega \to \pi^+ + \pi^- + \pi^0)} = 0.14 \pm 0.06.$$

It may be noted that Fig. 34 seems to confirm the existence of two peaks in the ρ region, one being the ρ, the other the 2π decay of the ω^0. We have no direct measure of the cross section for the process $\pi^- + p \to \pi^0 + n + \omega^0$, but we know that the process $\pi^- + p \to N_{3/2}{}^* + \omega^0$ dominates the reaction and consequently the rate should be slightly less than two times the cross section for $\pi^- + p \to \pi^- + p + \omega^0$. Thus, we deduce from the data in Fig. 34 that

$$(\omega \to \pi^+ + \pi^-)/(\omega \to \pi^+ + \pi^- + \pi^0) \geqslant 0.12 \pm 0.06.$$

Both of these values are greater by more than a factor

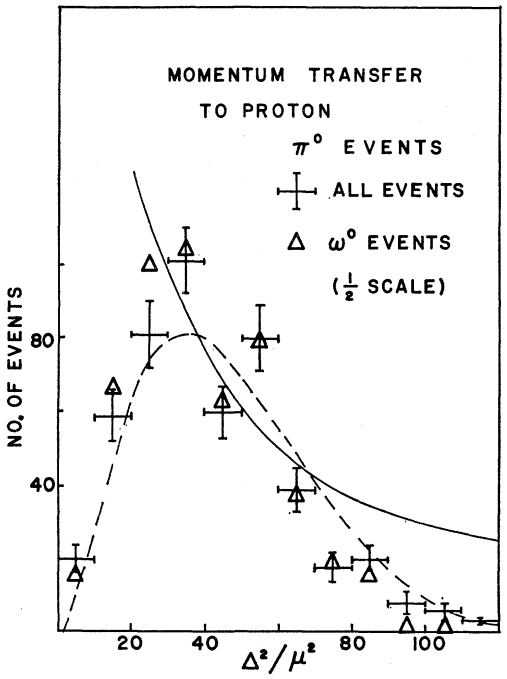

FIG. 35. Spectrum of momentum transfers to the proton for events of the type $\pi^- + p \to 3\pi + p + \pi^0$.

[22] A. N. Diddens, E. W. Jenkins, T. F. Kycia, and K. F. Riley, Phys. Rev. Letters **10**, 262 (1963).
[23] G. Feinberg, Phys. Rev. Letters **8**, 151 (1962).
[24] G. Feinberg, J. Bernstein, in *Proceedings of the 1962 Annual International Conference on High-Energy Physics at CERN*, edited by J. Prentki (CERN, Geneva, 1962), 170.
[25] S. L. Glashow, Phys. Rev. Letters **7**, 469 (1961).

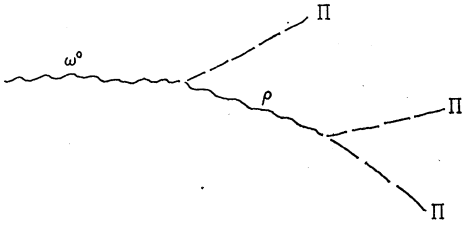

FIG. 36. Diagram of a decay mechanism for the ω^0.

of two than the value given by recent experiments at Berkeley looking at $K^-+p\rightarrow\omega^0+\Lambda^0$.[26]

Sakurai[27] has shown a method for determining the width of the omega from a measurement of the production cross section for the reaction $\pi^-+\pi^0\rightarrow\pi^-+\omega^0$. This cross section can be determined by applying the Chew and Low[28] extrapolation technique to the events wherein an omega is produced with low-momentum transfer. His calculation assumes that the decay of the omega proceeds through ρ intermediate states as indicated in Fig. 36. The $\rho-\pi-\pi$ coupling constant is determined from the width of the ρ, and the π^0 lifetime calculation can be used to determine the $\omega^0-\rho-\pi$ coupling constant. The total cross section for the above reaction at a given energy is directly proportional to the width of the ω^0. Figure 37 shows Sakurai's results for the calculation of the cross section assuming that the full-width of the ω^0 is 400 keV. Also shown is the unitarity limit for $l=1$. Using the data of this experiment for events with an ω^0 where the momentum transfer to the proton is less than 600 MeV/c and integrating the Chew and Low equation over the variable Δ^2, one obtains the points shown in Fig. 37. The slope of a line drawn through these points indicates that the ω^0 width may be of the order of 2.5 MeV but is not several times this. Figure 35 above has shown that there is no evidence in the momentum transfer spectrum that ω^0's are produced peripherally and, therefore, the method of experimentally determining the $\pi^-+\omega^0$ production cross section is probably not valid and merely sets a crude upper limit. Recently, Xuong *et al.*[29] and Bondár *et al.*[30] have obtained evidence for the peripheral production of the ω^0. The width indicated is of the order of 5 MeV. In the authors' opinion other diagrams may contribute to apparently peripheral processes and make this sort of estimate uncertain. One expects then that the result calculated from this experiment will give a cross section and hence a width which is an upper limit.

C. Other Multipion Resonances

Due to the rather large number of multipion states which have been reported, it is of interest to mention those for which effects were not seen in this experiment. Samios *et al.*[19] have presented data which claim to show the presence of two resonances in the $\pi^+\pi^-$ mass spectrum at 395 and 520 MeV in the π^0 and neutron event types. Their beam momentum was 4.7 BeV/c. As can be seen in Figs. 14 and 25, there is no indication that either of these states contribute to the data presented here. Some slight evidence for a bump at 450 MeV may be seen in Fig. 34.

The ξ, first seen by Barloutaud *et al.*[31,32] is proposed to be a $T=1$ resonance with a mass of 575 MeV decaying into a pair of pions. This was seen in the proton, π^+, and π^0 final state in an experiment using a π^+ beam at energies of 820, 900, and 1050 MeV. The $\pi^+\pi^0$, $\pi^-\pi^0$, or $\pi^+\pi^-$ mass spectra do not show any indication of this state. Also, the decay mode $\omega^0\rightarrow\xi+\pi$ is allowed but not seen.

Evidence for a $T=2$ di-pion resonance has been presented by Biswas *et al.*[33] in data obtained by means of a 4-BeV/c momentum π^- beam. The $T=2$ state was seen in four-pronged events with a π^0 or neutron at a mass of 620 MeV. They did not see the formation of this state for $3\pi+p$ events, since for these the main contribution was due to the ρ. The $T=2$ state was also suppressed for events with an ω^0. The experiment re-

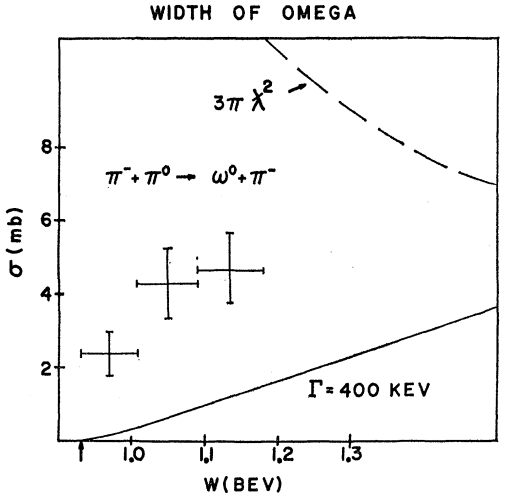

FIG. 37. Cross section $\pi^-+\pi^0\rightarrow\pi^-+\omega^0$ as deduced from events $\pi^-+p\rightarrow\omega^0+\pi^-+p$.

[26] J. Shafer, J. Murray, M. Ferro-Luzzi, and O. Huwe, International Conference on Nucleon Structure, June, 1963 (unpublished); W. J. Fickinger, D. K. Robinson, and E. O. Salant, Phys. Rev. Letters **10**, 457 (1963). The results are, however, consistent with results from the Wisconsin group reported by W. D. Walker at the CERN Conference in 1962.

[27] J. J. Sakurai, Phys. Rev. Letters **8**, 300 (1962).

[28] G. F. Chew and F. R. Low, Phys. Rev. **113**, 1640 (1959).

[29] N. Xuong, R. L. Lander, W. A. W. Melhop, and P. M. Yager, Phys. Rev. Letters **11**, 227 (1963).

[30] L. Bondár, E. Keppel, G. Kraus, W. P. Dodd, B. Tallini, G. Wolf, I. Butterworth, F. I. Campayne, M. Ibbotson, N. N. Biswas, I. Derado, D. Luers, and N. Schmitz, Phys. Letters **5**, 209 (1963).

[31] R. Barloutaud, J. Heughebaert, A. Levegue, J. Meyer, and R. Omnes, Phys. Rev. Letters **8**, 35 (1962).

[32] B. Sechi Zorn, Phys. Rev. Letters **8**, 282 (1962).

[33] N. N. Biswas, I. Derado, K. Gottstein, V. P. Kenney, D. Luers, G. Lutgens, and N. Schmitz, Phys. Letters **3**, 11 (1962).

ported here shows no evidence for a $T=2$ state at 620 MeV in any of the event types.

In p-p collisions at an energy of 2.0 BeV, Pickup *et al.*[34] have found evidence for a three-pion resonance at a mass of 625 MeV. It is seen in the $\pi^+\pi^-\pi^0$ and $\pi^+\pi^+\pi^-$ spectra, so it must have $T=1$, 2. A state called α has been proposed by Dennery and Primakoff[35] to have $T=1$ and $J=1^{+-}$ and a mass between 400 and 600 MeV. This state is proposed to be important in determining the axial-vector form factor involved in strangeness conserving baryon-lepton weak interactions. The $T=1$ three-pion mass spectra presented in this work do not show any indication of the presence of this state.

One of the peculiar features of the data presented here seems to be the apparent interference between the "classical" 3,3 resonance at 1250 MeV and the $I=\frac{3}{2}$ resonance at 1920 MeV. In the authors' opinion this is a real effect since the excitation of the 1920-MeV level also shows up in reaction channels not discussed in this paper. Namely in the process $\pi^-+p\rightarrow\pi^-+\pi^++n$, the π^-n mass spectra shows an interference at 1900 MeV. Also the reaction $\pi^-+p\rightarrow\Sigma^-+K^0+\pi^+$ seems to show the effect in the Σ-K mass spectrum. The sort of picture that this produces is that the crossing diagram of the type shown below in Fig. 38 is of considerable importance. In the case of the process $\pi^-+p\rightarrow\pi^-+\pi^-+p+\pi^+$ the amplitude for the above process would interfere with the more usual one-pion exchange process. This interference could result in the apparent split of the $I=\frac{3}{2}$, $J=\frac{3}{2}$ bump in the π^+p spectrum.

Note added in proof. Recently a group at Saclay [Bareryre *et al.*, Phys. Letters 8, 137 (1964)] has pointed out what seems to be evidence for a resonance in the $I=\frac{1}{2}$, $J=\frac{1}{2}$ π-nucleon state. The effect of this resonance should appear most clearly in the events $\pi^-+p\rightarrow$

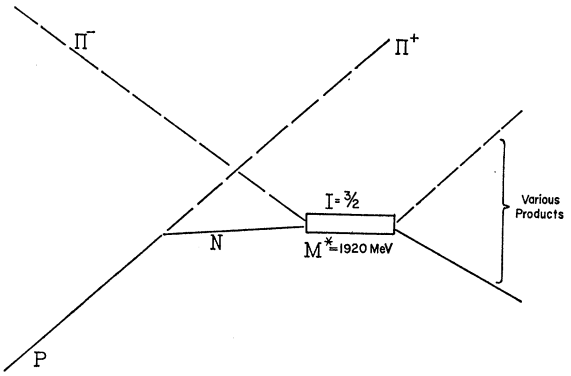

FIG. 38. A possible diagram contributing to $\pi^-+\pi^++n$ production in π^-+p collisions.

$\pi^-+\pi^-+\pi^++p$ for which the π^++p are not resonating in the 3, 3 state. Indeed if one examines our Fig. 6 there seems to be evidence for a peak in the π^--p system at 1400 MeV. The $I=\frac{1}{2}$, $J=\frac{3}{2}$ at 1500 MeV also seems to show on the same plot. Thus our data are consistent with the conclusions of the Saclay group, as they have pointed out.

ACKNOWLEDGMENTS

The authors are indebted to many people for their efforts in the work presented here.

The members of the Walker-Erwin bubble-chamber group have all contributed in many ways to the completion of this experiment.

The help of Dr. H. Fechter and D. Lyon in the early stages of this work were greatly appreciated.

Over the course of the experiment the following scanners, whose help has been invaluable, contributed many hours to this project: K. Eggman, C. Seaver, E. Horowitz, S. Rieder, T. Eblen, A. Rodland, W. Gundlach, D. Ebert, F. McElroy, and J. Highland.

The University of Wisconsin Numerical Analysis Laboratory has provided computer time on the 1604.

[34] E. Pickup, D. K. Robinson, and E. O. Salant, Phys. Rev. Letters 8, 329 (1962).

[35] P. Dennery and H. Primakoff, Phys. Rev. Letters 8, 350 (1962).